

## **Università Degli Studi Di Padova**

Dipartimento di Geoscienze

Direttore Prof.ssa Cristina Stefani

**Tesi Di Laurea Magistrale In Geologia E Geologia Tecnica**

Progetto in collaborazione con ENI s.p.a.

### **3D GEOLOGICAL MAPPING AND RECONSTRUCTION OF DOLOMITE DISTRIBUTION ACROSS THE VENETIAN PREALPS BETWEEN VALDOBBIADENE AND SAN BOLDO PASS (SOUTHERN ALPS, ITALY)**

**Anno Accademico 2017/2018**

Relatore: Prof. Nereo Preto

Correlatori: Dott. Marco Franceschi

Tutor ENI: Dott.ssa Ornella Borromeo

Laureando: **Giordano Salvetti**

*...Dedicata ai miei genitori*

## Index

<b>1. Introduction</b>	<b>p. 6</b>
1.1. Geological setting	p.8
1.2. Jurassic paleogeography and the Belluno Basin	p.9
1.3. Stratigraphy	p.13
1.4. Tectonic evolution 1: Mesozoic rifting	p.19
1.5. Tectonic evolution 2: Alpine Compression	p.21
1.6. Dolomitization	p.27
<b>2. Methods and material</b>	<b>p.29</b>
<b>3. Data collection</b>	<b>p.30</b>
<b>4. Geological map and description</b>	<b>p.32</b>
4.1. Improvements of the geological map	p.34
4.2. The Col Visentin - Monte Garda anticline	p.36
4.3. Mapping of the dolomitized area	p.39
<b>5. Topographic model</b>	<b>p.42</b>
5.1. Geological modeling with Skua Gocad	p.44
5.1.1. Geological cross sections	p.45
5.1.2. Generation of boundary surfaces	p.46
5.1.3. The geologic grid of the anticline structure	p.51
5.1.4. Features of the Col Visentin - Monte Garda anticline	p.56
5.2. Gaussian curvature	p.57
5.3. Geostatistical distribution of the dolomitization	p.59
5.4. The 3D representation of the dolomitization front	p.62
5.5. Volume of the dolomitized rocks	p.66
<b>6. Discussion</b>	<b>p.69</b>
6.1. Dolomitization/faults relationships	p.69
6.2. Detection of a blind back thrust in the NE sector	p.72
6.3. Gaussian curvature and dolomitization	p.73
6.4. Comparison with analog structure in the subsurface	p.74
<b>7. Conclusion</b>	<b>p.78</b>
<b>8. Bibliography</b>	<b>p.80</b>
<b>9. Thanks</b>	<b>p.84</b>



## **Abstract**

Structural traps created by compressional tectonics can hold very interesting hydrocarbon accumulations, and are one of the main targets for hydrocarbon exploration. In a particular geological/tectonic setting, the faults generated by compression events could favor the circulation of dolomitizing fluids leading to the formation of fault related dolomitized bodies that can strongly improve the porosity and permeability of the parent rock or sediment. The prediction of the dolomite distribution and the relationships between faults and dolomitization may result difficult using only indirect methods of investigation as seismic prospection. This thesis is aimed at producing the 3D geological model of the dolomitized Col Visentin - Monte Garda anticline that could be compared with a plausible subsurface analogue. The whole area of the Southern Alps was extensively affected by Alpine compression. The tectonic structure of the Col Visentin - Monte Garda is the product of this tectonic phase. The dolomitization in this region is attributed to the circulation of dolomitizing fluids along the main faults, occurred during the Miocene.

In this work of thesis a geological map and a 3D geological model of the structure were produced. The distribution of dolomitized rocks was then reconstructed, on the base of discontinuous field data, with geostatistical methods. The dolomitization and its relationships with the tectonic evolution on the Col Visentin - Monte Garda anticline were then investigated. The results were then compared with an analogue which has similar tectonic and dolomitization characteristics.

# 1 Introduction

In the last years, the decreased discoveries of hydrocarbon reservoirs has lead to exploration toward different kinds of reservoirs (Møller-Pedersen & Koestler, 1997; Coward et al., 1998) as those related to dolomitization. In this work, a case of dolomitization and its potential as a reservoir analog have been examined. The relation between dolomitization and the structural control have gained increased attention worldwide (e.g., Davis and Smith, 2006).

It is well known that some dolomitization processes can substantially improve rock porosity and permeability (e.g., Quig Sun, 1995) which are two of the main characteristics to determine the reservoirs potential. Once formed, the dolomite preserves its permeability and porosity much better during burial than limestone, due to its greater ability to resist the pressure solution (Warren et al., 2000). Not all dolomites make good reservoirs, because porosity depends on their original depositional fabric and the nature and volume of dolomitizing fluids. Nevertheless, approximately 80% of the recoverable oil in North America is stored in dolomite reservoirs (Warren et al., 2000).

The Southern Alps were interested by different dolomitization phases during the Alpine compression. Many studies were done in order to understand the properties and distribution of the dolomitization (e.g., Ronchi et al., 2012, Zempolich & Hardie, 1997).

This study was aimed at the reconstruction of the dolomitization front in the Col Visentin - Monte Garda anticline, a tectonic structure in the Treviso and Belluno prealps having dimensions comparable to the scale of many carbonate reservoirs. The 3D modelling integrated with the geological map and geostatistical methods allowed to answer the following questions:

Does a relationship between the fault network and the stratigraphic heights reached by the dolomitization exist?

Is the Gaussian curvature correlated to the areas of maximum dolomitization height?

How does the 3D geological model of the Col Visentin - Monte Garda compare with a real analogue reservoir?

## 1.1 Geological setting

The area of study is located in the Belluno basin between Valdobbiadene and San Boldo Pass in the southernmost part of the Southern Alps, which represent the south vergent sector of the Italian Alpine chain, separated from the north-vergent sector by the Insubric Line (Periadriatic Lineament). The Southern Alps are made up of a complex Permian to Neogene sedimentary succession, which rest on a Ercinian metamorphic basement.

The sedimentary formations of the Belluno basin are synrift deposits correlated to the Mesozoic extensional tectonic, successively deformed by Alpine compressional events. These sediments come from two nearby Jurassic carbonate platforms, the Friulan platform to the East and the Trento platform to the West. The basin stratigraphy s sedimentary sequence resting on top of the Dolomia Principale Formation (Late Triassic) and made of the Soverzene Formation (Hettangian-Toarcian), Igne Formation (Toarcian-Bajocian) (Masetti & Bianchin, 1987; Jenkyns & Clayton, 1986; Jenkyns, 1988) and Vajont Oolitic Limestone (Bajocian-Callovian) (Casati & Tomai1996). This last unit connects the two platforms with a turbiditic sediment ramp (Bosellini & Masetti, 1972; Bosellini et al.,1981). Above the Oolitic limestone the Fonzaso Formation was deposited (Bathoniano sup-Titoniano inf) (Cobianchi, 2002; Bosellini et al., 1981b).



## 1.2 Jurassic paleogeography and the Belluno Basin

The area of interest is part of the Col Visentin - Monte Garda Anticline within the Belluno Basin. During the Jurassic, it was filled with pelagic-hemipelagic succession with sediments coming in part from the edges of the two nearby platforms.



**Fig1:** Picture from Google Earth. The whole study area between the two provinces of Belluno, in the North portion of the picture, and Treviso, in the South.

The Belluno Basin is placed in the eastern portion of the Southern Alps in the North of Italy. Subsurface data from ENI (well logs and seismic lines) permitted to estimate the dimension of the Belluno Basin, which was 30 km wide and more than 100 km long, gradually narrowing southwards, and extended westward and eastward toward the city of Belluno (Bosellini et al.,1981). The southern margin of the Belluno Basin (Masetti et al., 2012) was North of Venezia and corresponds to the north-western edge of the North-Adriatic basin, developed in the middle Jurassic.

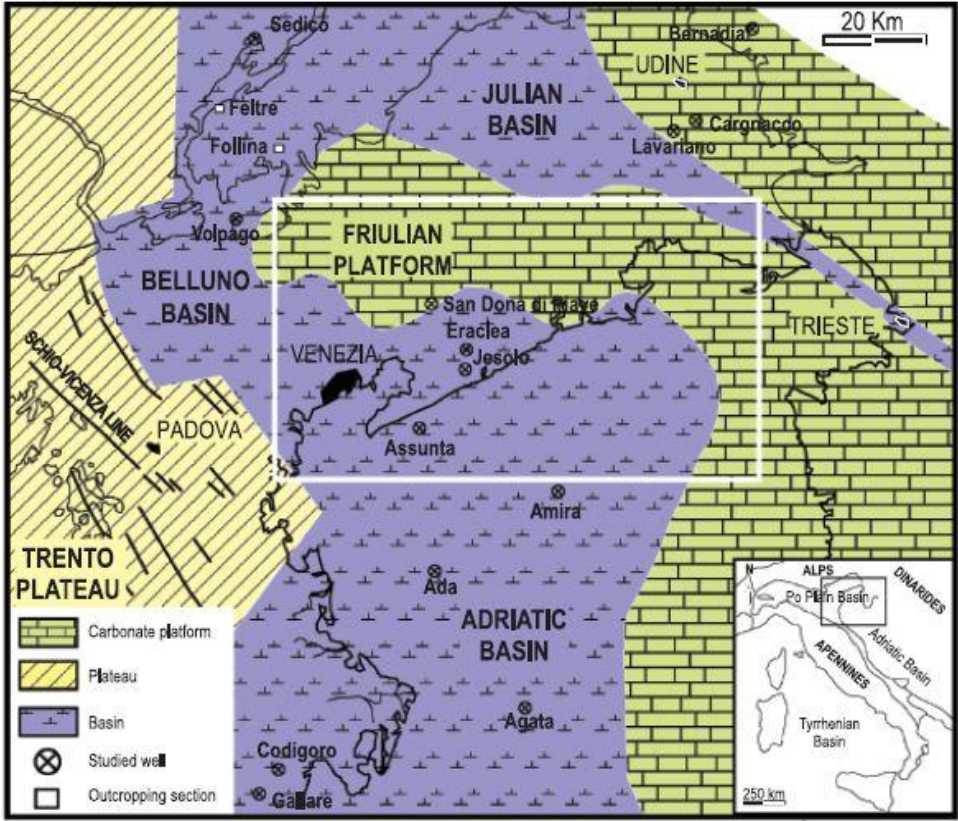


**Fig 2:** From Mancin, A & Di Giulio 2009. Shows the Mesozoic Paleogeography of the Venetian–Friulian area on the actual geography of the N-E Italy.

The Belluno Basin is bordered by Permian-Mesozoic normal faults resulted from the rifting that preceded the North Atlantic Ocean opening. A system of extensional structures produced a horst and graben geometry that deformed a pre-existent peritidal platform, of the Principal Dolomite. This Mesozoic rifting phase has conditioned the sedimentation in the whole area of the Southern-Alps.

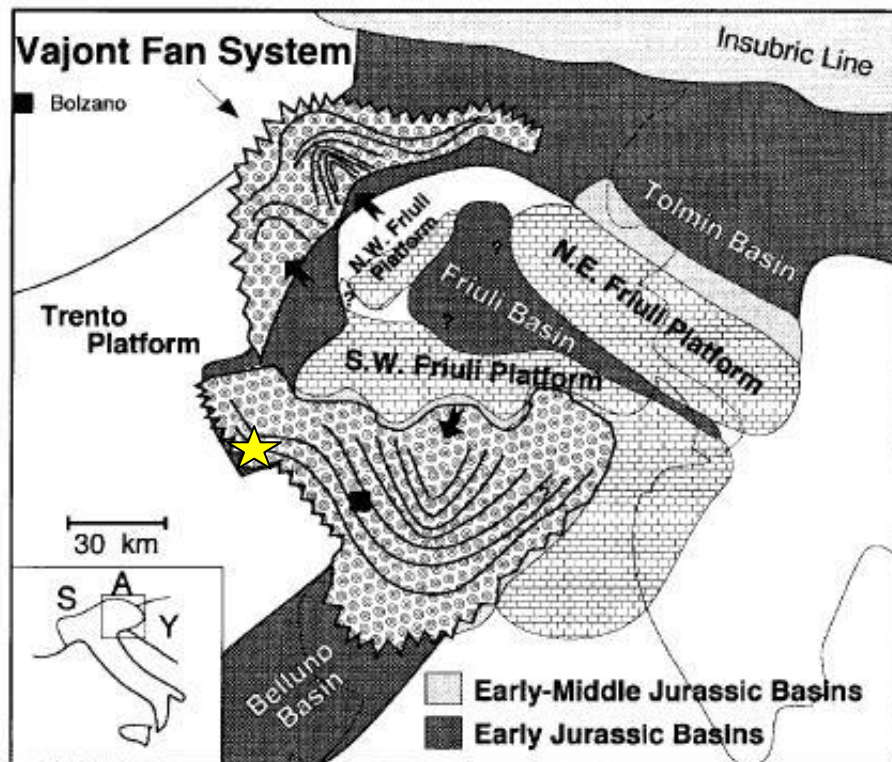


**Fig 3:** Facies map of the Belluno Basin (modified from Zempolich & Hardie, 1997). The yellow star localizes the paleo-position of the study area during the activity of the Belluno basin.

West of the Belluno Basin, the Trento Carbonate Platform is made up by the thick sequence of the Calcarei Grigi Group (Early Jurassic). This unit was deposited in a peritidal, shallow water environment (Masetti et al., 1996; Winterer & Bosellini 1981).

East on the Friuli Platform, during the Middle Jurassic, oolitic shoals were forming, and ooids were redeposited westward as turbiditic flows, that filled the Belluno Basin (Vajont Oolitic Limestone) (Bajocian - Bathonian).

The western boundary of the Vajont Oolite corresponds to the eastern edge of the Trento Platform. As the sediments were filling the basin, the roughness due to the faults of Mesozoic rifting was smoothed. This allowed the connection of the two platforms by a gently inclined depositional surface (Bosellini & Masetti 1972; Bosellini et al., 1972b).

### 1.3 Stratigraphy

The stratigraphy of the Belluno Basin includes the Soverzene Formation (Hettangiano - Lower Pleisbachiano), followed by the Igne Formation (Toarcian), the Vajont Oolitic Limestone (Bajocian - Bathonian), the Fonzaso Formation (Bathoniano sup - Titoniano inf), the Maiolica Formation (Late Tithonian - Early Aptian) and the Scaglia Variegata Alpina (Aptian - Cenomanian).

#### SOVERZENE FORMATION (Hettangian - Toarcian)

The Soverzene Formation is made up by a succession of gray-brown dolomite layers, 20 - 40 cm thick, associated to yellow-grey flint nodules. The lower part of the unit is rich in organic matter, while in the whole formation many discordant bodies of intraformation breccias with crystalline dolomitic matrix are present. Where the unit was not dolomitized, radiolaric mudstone and wackestone with sponge spicules occur. The unit does not crop out in the study area.

#### IGNE FORMATION (Toarcian - Aalenian)

The Formation is characterized by various lithologies. A typical facies is an alternation of dark-grey, dark-brown marl layers, 10 - 20 cm thick, and grey, dark-grey limestone, less than 10 cm thick (e.g., Riva et al., 1980). A cyclic alternation is observed every 50 cm between silty and marly layers and black shales with fish remains and high content of organic matter, in agreement with a low oxygen basinal depositional setting (Casati & Tomai, 1969)

During the survey the black-shales of the Igne Formation were not found, but an alternation between dark-grey marls and dark-green, grey chert, nodules or thin discordant layers were commonly observed, in the limestone on the top of the formation in contact with the lower Vajont Oolitic Limestone boundary.

## VAJONT OOLITIC LIMESTONE (Bajocian - Bathonian)

This formation is composed of gray, light brown, poorly sorted oolitic packstone-grainstone in banks of 1 to 5 m, with coarsening upwards gradation. In the lower part of the banks, intraclastic breccias with oolitic matrix may be present. Locally the lower Vajont Oolite is marked by the presence of thin chert layers. The Vajont Oolitic Limestone is often replaced by saccaroid and porous dolomite. This unit was interpreted as ooids being formed in shallow water settings and resedimented in deep water as turbidities, forming the slope of the adjacent Friulan Platform (Bosellini et al.,1981). Zempolich and Hardie (1997) suggest that the Vajont Oolitic Limestone was deposited during the latest Aalenian-earliest Bajocian and is an eastward thickening wedge, formed on a depositional area in excess of 100 km along strike and 50 km across strike. Along the western edge of the Belluno Basin, slope and basinal sediments of the Vajont Oolitic Limestone onlap downfaulted blocks and margins of the east Trento platform (Bosellini et al., 1981).



**Fig 4:** An outcrop of the undolomitized Vajont Oolitic Limestone, detected in the study area.

## FONZASO FORMATION (Callovian - Kimmeridgian)

The Fonzaso Formation is composed by finely stratified micritic and bioclastic limestone, alternated with chert layers. The amount of chert and its shape changes from the base to the top of the formation and occurs initially as chert nodules, and as horizons of 15 - 20 cm thick toward the top. The depositional environment is similar to the Vajont Oolitic Limestone but, instead of the oolitic sediments, the grains are skeletal from the turbiditic flows developed on the eastern edge of the Friuli Platform. The aforementioned platform underwent emersion during the Callovian - Bathonian, while during the Oxfordian the platform was interested by a new marine transgression, which permitted the establishment of reefs. On the top of the formation there is a progressive decrease of the bed thickness and of the amount of chert, whereas the limestone starts to be alternated to dark gray silt and clay layers with no organic matter (Martins & Fontana, 1968). In the central Belluno Basin the Fonzaso Formation grades upward into nodular micritic red limestone belonging to the upper Rosso Ammonitico (Kimmeridgian - Tithonian). The boundary with the underlying Vajont Oolitic Limestone corresponds to the disappearance of oolitic turbidites (Martins & Fontana, 1968). The Fonzaso Formation is slightly thickening westward in the study area.



**Fig 5:** An outcrop of the Fonzaso Formation near Follina.

## MAIOLICA (Late Tithonian - Early Aptian)

The Maiolica formation consists of pelagic mudstone-wackestone containing radiolarians and sponge spicules. In the Grappa massif, the whole pelagic Cretaceous succession is locally cut by neptunian dykes, filled by breccias made of clasts of pelagic micrite and chert nodules, embedded in a micritic matrix. Most of these dykes are dolomitized (Ronchi et al., 2012).

The Maiolica is composed by a prevalence of micritic, light-gray or rarely light-brown limestone, with abundant silt-clay intercalations and chert nodules and horizons. The chert has different colors, from black to green and red, and it can be found as nodules or layers less than 30 cm thick (Baudin & Faraoni, 1998).

The thickness of the layers is variable and decreases upward from 50 cm, to less than 10 cm. In the Belluno Basin and in the whole area of the Southern Alps, the thickness of the Maiolica is always less than 400 m. In the central portion of the Belluno Basin, the base of the Maiolica lies on an atypical Rosso Ammonitico, having abundant grey silt. The upper boundary of the Maiolica is gradational with the Scaglia Variegata Alpina.



### SCAGLIA VARIEGATA ALPINA (Aptian - Cenomanian)

The Scaglia Variegata Alpina is a limestone with abundant silt and clay interlayers, chert nodules and decimetric layers of limestone with light gray-light pink colors. In some portions of the Belluno Basin, it shows light/dark green colors of the limestone.



**Fig 6:** The Bonarelli horizon, detected in the Quero Valley, marks the boundary between the Scaglia Variegata Alpina and the overlying Scaglia Rossa

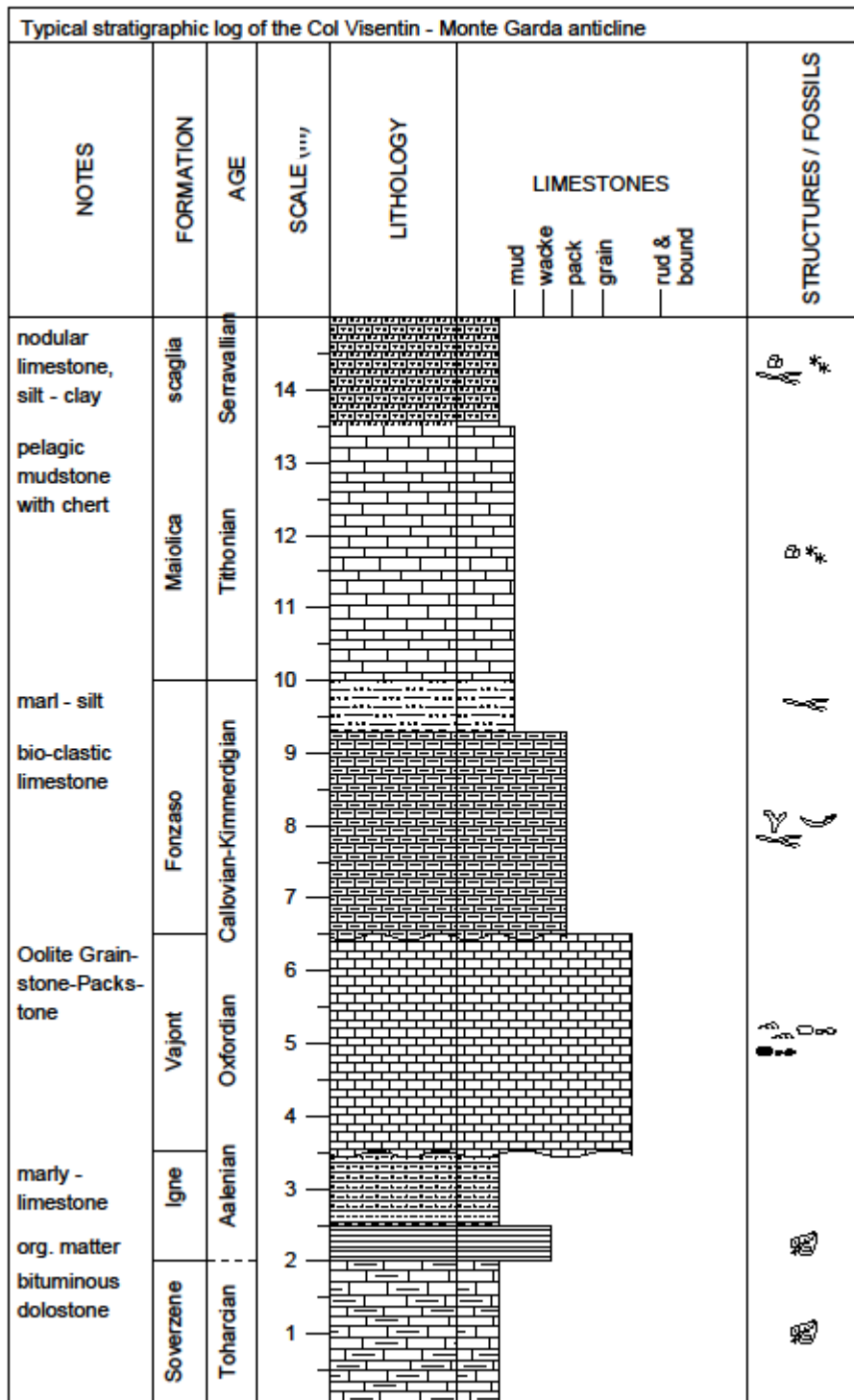


**Fig 7:** Stratigraphic log representing the main lithologies and their thickness of the area of study (scale 1:10.000).

## 1.4 Tectonic evolution 1: Mesozoic rifting

The Southern Alps belong to a portion of a Jurassic passive margin, on the north-western edge of the Adriatic Plate (Winterer & Bosellini, 1981). The present tectonic setting of the area is due to different structural phases. The Mesozoic rifting phase was related to the opening of Ligure Piemontese Ocean, with the imposition of normal faults setting with strike (N10°W-N10°E) (C. Doglioni et al., 1987). The normal faults divided the pre-existing peritidal platform, the Triassic Dolomia Principale, in blocks. The Southern Alps area on the whole was divided in four domains. Starting from the west, there were the Lombardy Basin, the Trento Platform, the Belluno Basin and in the most Eastern part the Friulan Platform (Castellarin, 1972, Doglioni & Bosellini, 1987).

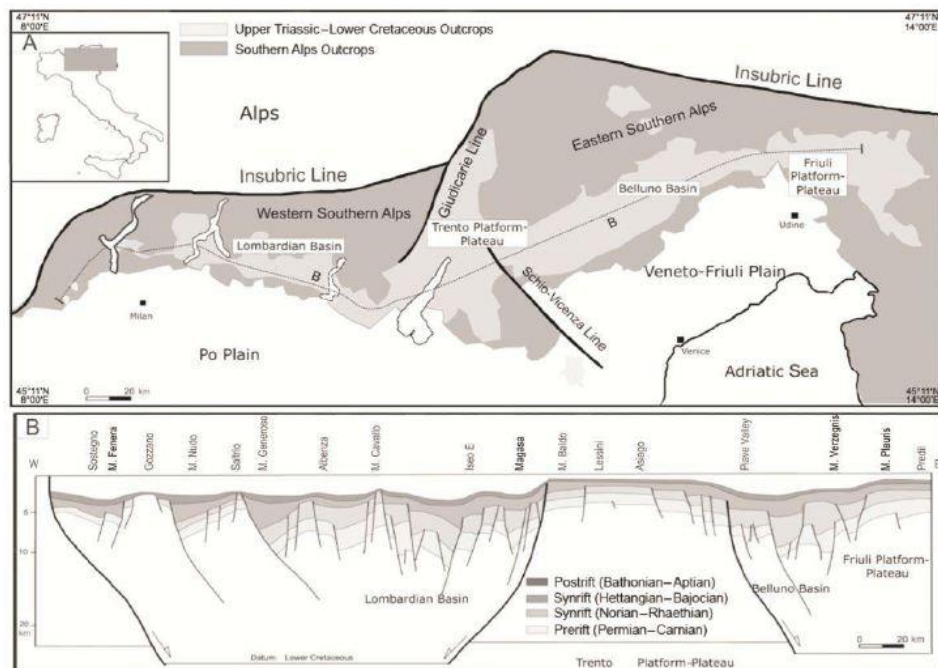


**Fig 8:** Modified from Doglioni 2006. This picture represents a cross section of the Southern Alps, with the four main Jurassic structural domains due to the horst and graben geometry.

The normal faults attributed to the Mesozoic rifting phase have a E-W to SE-NW strike and separate domains (horsts and grabens) with different rates of subsidence (Masetti et al., 2012) which have permitted many variations in thickness of the Jurassic successions. Some spectacular examples of this tectonic phase are exposed on the Trento Platform in the Calcarei Grigi Group (Martinelli et al 2017). The whole Mesozoic sequences can be fully or partially dolomitized. An example is the study area, where the Jurassic units involved in the anticline structure of the Col Visentin - Monte Garda show various degrees of dolomitization (Zempolich & Hardie, 1995).

## 1.5 Tectonic evolution 2: Alpine compression

The Eastern part of the Southern Alps is a structural belt located South of the Periadriatic Lineament, and affected by intensive south-vergent thrusting, opposite to the Northern Alpine chain which is north-vergent (Castellarin et al., 2000). The second main tectonic event in this area was a North-South compression, caused by the collision between Europe and Africa, which led to the formation of the Alpine chain. Some authors (e.g., Castellarin et al., 2010; Doglioni et al., 1987) suggest that the compressional event in the Southern Alps can be divided in three different stages: **Eo-Alpine** before the early Miocene, **Meso-Alpine** during the early Miocene, (**Neo-Alpine**) during Messinian. The Venetian part of the Southern Alps (North-East Italy) is a south vergent thrust belt, that mostly formed during the Neogene; the shortening of the Southern Alps in this part is of at least 30 km. The thrusts trend ENE - WSW and are superimposed on a set of inherited N-S trending normal faults of the Mesozoic rifting (Winterer & Bosellini, 1981).

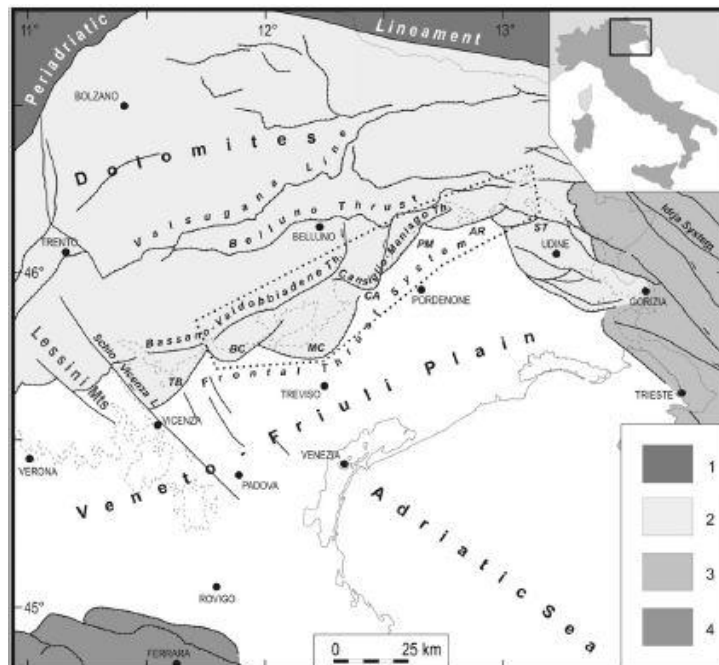


**Fig 9:** From Doglioni 2006. Main lineaments of the Eastern Southern Alps.

These inherited structures strongly controlled the following thrust belt. According to Doglioni (1987), the geometry of the thrust belt is similar to an imbricate section of sedimentary fan, with a main envelope angle produced by thrust slices close to  $7^\circ$ , critical taper of wedge in according to the model of Platt 1988.

The structural evolution of the thrust belt shows a general rejuvenation from the internal thrusts to the external ones (Fig. 10). Some internal thrust sheets seem to have been reactivated also in recent times (Sleyko et al., 1987; Doglioni et al., 1992).

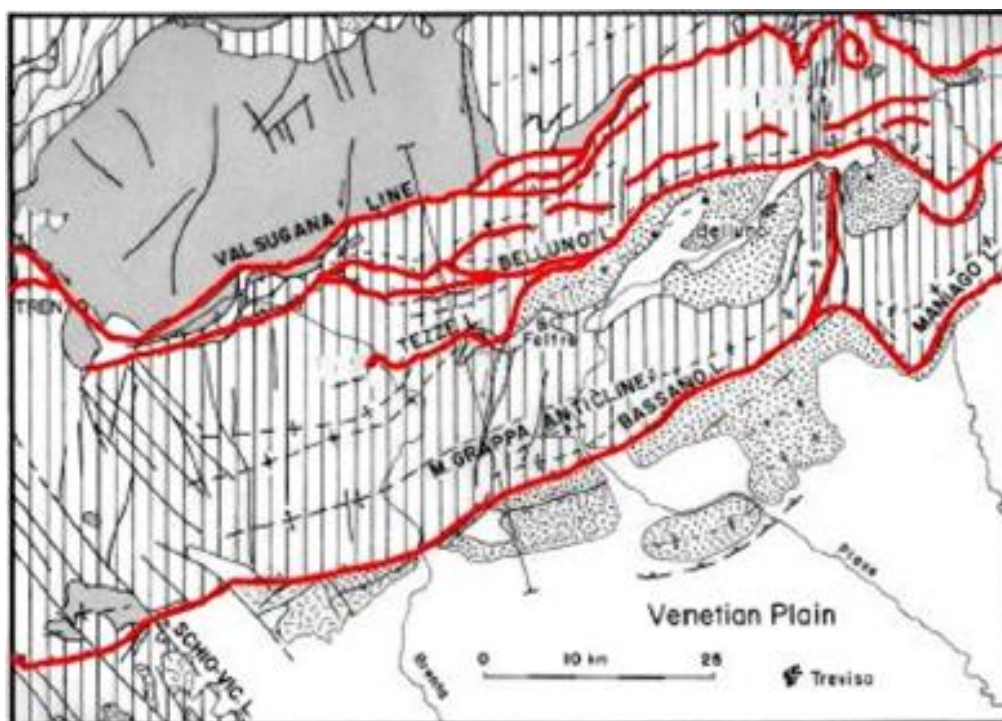


**Fig 10:** Modified from Doglioni, 1992. This picture shows the main South Alpine thrusts that are subject to rejuvenation.

## 1° First phase (Eo-Alpine)

The first compressional tectonic event probably began during the Late Oligocene (Chattian) (Mancin et al., 2007; Caputo et al., 2010) and evolved during the Early Miocene (Aquitanian - Buldigardian), generating the Insubric Line or Periadriatic Lineament (Massari, 1990; Castellarin et al., 2007; Caputo et al. 2010). The maximum compressional axis ( $\sigma_1$ ) associated with this event was oriented NNE - SSW and the  $\sigma_3$  was sub-vertical. This implied that the inverse faults followed an entirely Andersonian behaviour (Castellarin et al., 1992, Caputo, 1996, Caputo et al., 2010). Since the Miocene (Langhian), the central and Southern Veneto and Friuli areas represented a distal foreland basin characterized by a regional monocline dipping northwards, with angles less than 1°, filled by terrigenous-carbonate deposits (e.g. Massari et al., 1986; Fantoni et al., 2002, Caputo et al., 2010).

## 2° Second phase (Meso-Alpine)

The second compressional phase in the Eastern Southern Alps began during the early Miocene (Serravallian). During this time the Valsugana thrust and the Belluno thrust system were formed, and progressively propagated Southward (Doglioni, 1990, 1992; Massari et al., 1993; Carulli e Ponton, 1993; Caputo, 1997; Castellarin et al., 1992, 1996, 2002a; Selli, 1998; Neri et al. 2007; Caputo et al., 2010). The contractional structures are characterized by ramp flat ramp geometries, with average ENE-WSW strike and SSE direction of slip vectors. The maximum compression axis is oriented NNW - SSE (Castellarin et al., 1992; Caputo, 1996, 2010). Fission track studies on sediments of the Venetian Foreland Basin have shown that the fastest exhumation rates occurred in the Tortonian, the uplift was likely due to rapid growth and migration of the Southern Alpine Fold-and-Thrust belt (Fantoni et al., 2002; Barbieri et al., 2004; Zanferrari et al., 2008; Caputo et al., 2010). The sediment column for the central portion of Venetian Foreland Basin exhibits a thickness of 2500 m, mostly of this being made of lithic carbonate sand and carbonate pebbles from the erosion of the early Southern Alps.

### 3° Third phase (Neo-Alpine)

This third compressional phase has led to a gradual change of the direction of compression, while the sedimentation into the foredeep continued undisturbed. This was probably the strongest of the three compressional phases, and is dated Messinian - Pliocene (Castellarin et al., 1992, 2006a; Cantelli & Castellarin, 1994; Caputo 1996; Caputo et al., 1999; Castellarin & Cantelli 2002; Caputo et al., 2010). This phase is characterized by a NW-SE direction of maximum horizontal compression.

During this phase in the Dolomites, located in the internal sector of the Southern Alps, sub-vertical strike-slip faults systematically dislocated the older low-angle E-W compressional structures (Caputo, 1997; Caputo et al, 1999; Neri et al., 2007; Caputo et al., 2010).

In the external sector of the Southern Alps, the tectonic regime remained purely compressional ( $\sigma_3$  was vertical) and determined a complex contractional pattern mainly represented in the area of study by the Bassano - Valdobbiadene Thrust with prevalent strike trajectory ENE-WSW. This compression also produced the anticline-fold in front of the thrust and blind-thrusting (Fig.11) (Doglioni, 1990a, 1992; Carulli & Ponton, 1993; Caputo, 1994; Castellarin et al., 1998, 2006b; Schöborn, 1999; Zanferrari et al., 2008; Caputo et al., 2010).



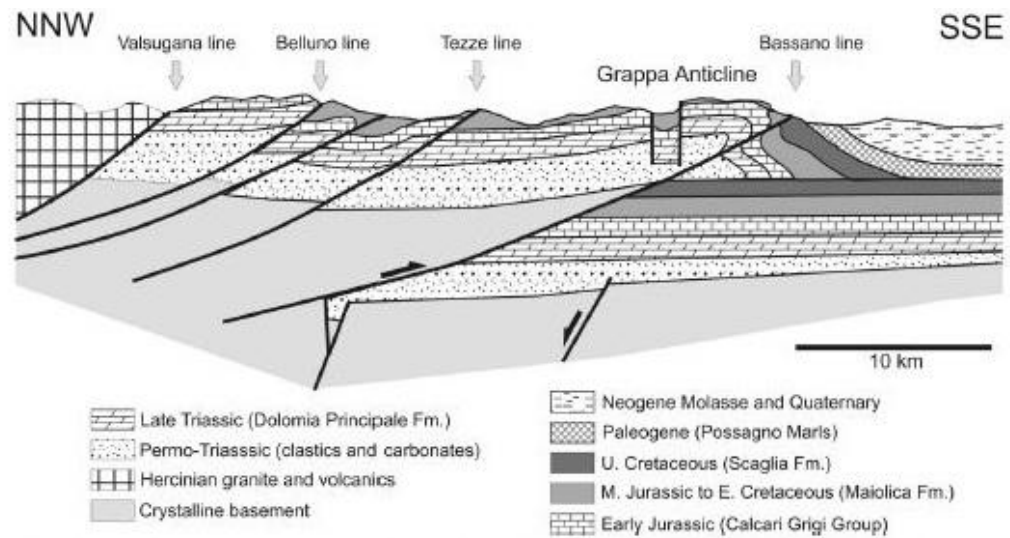
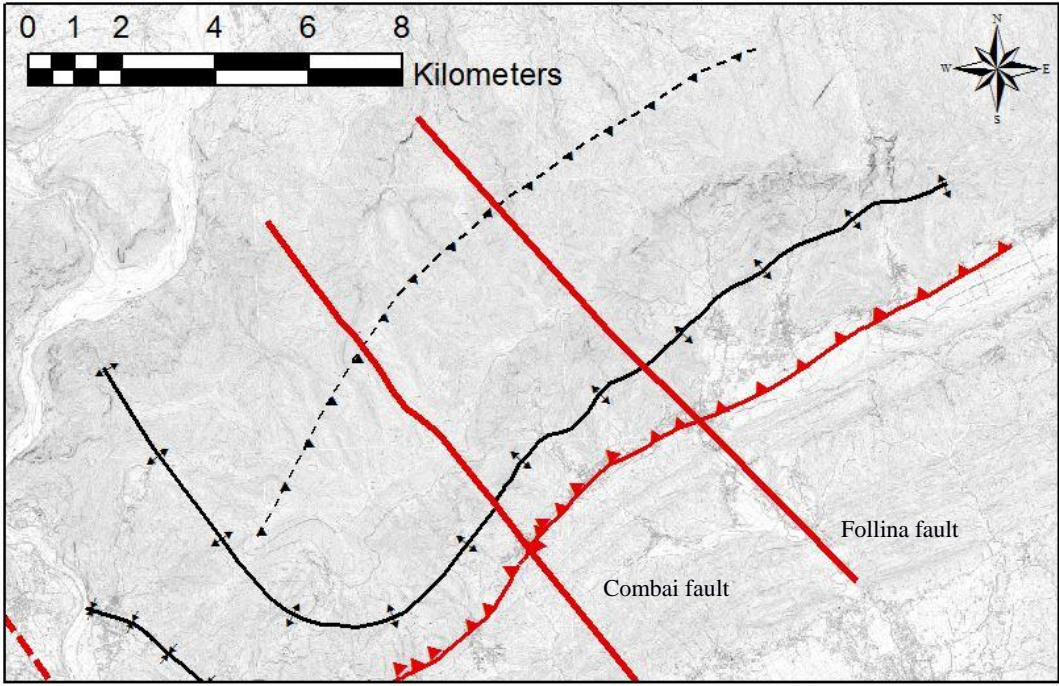


**Fig 11:** Modified from Ronchi et al., 2012. Schematic geological map showing the main thrusts and tectonic lines in the Venetian Alps. This geological cross-section is passing through the Monte Grappa Anticline.

The Col Visentin - Monte Garda fold is a strongly asymmetric, south-vergent anticline which is the main object of this work. It is bound to the west by a strike-slip lineament across the Quero Valley (Fig. 12). This lineament developed due to the reactivation of a Mesozoic normal fault, belonging to the rifting phase, during the Messinian-Pliocene Adriatic compressional event. It has the same direction of the strike-slip Schio-Vicenza fault ( $N^{\circ} 310^{\circ}$ ), which main activation phase is dated to the Messinian-Pliocene.

The Neo-Alpine compression has also produced SE vergent folds and thrusts, to which the Col Visentin - Monte Garda anticline fold belongs. Its main strike is NW-SE. The paleostress directions obtained by meso-structural analysis are oriented NW-SE with prevailing values of  $N^{\circ} 300^{\circ}$  and  $N 330^{\circ}$  (Castellarin & Cantelli, 2000).

The Bassano - Valdobbiadene thrust and the Montello thrust could represent the most recent compressional structures in the whole Southern Alps, and may account for a total upper crustal shortening of up to 20 km (Castellarin & Cantelli, 2000). The footwall of the Col Visentin - Monte Garda anticline, from Valdobbiadene to San Boldo Pass, shows a slickenside due to the thrust action, with a steep angle 35° - 40°.



- Legend**
- Combai-fault
  - Follina-fault
  - ▲- Blind-back-thrust
  - - - Quo-ro-strike-slip
  - ▲ Anticline
  - ▲ Thrust Bassano-Valdobbiadene
  - ▼ Syncline

**Fig 12:** Representation on the topography of the main tectonic lineaments coming from the survey and literature.

## 1.6 Dolomitization

There is a growing interest for dolomitization due to fact that many hydrocarbons reservoirs are into dolomitized rocks bodies (e.g., Purser et al., 1994; Braitwaite et al., 2004; Ronchi et al., 2012). Many portions of the Southern Alps have been dolomitized, as the present area of study. During the survey on the Col Visentin - Monte Garda anticline many zones with different degree of dolomitization were detected and dolomitization reaches different stratigraphic quotes within the Jurassic succession (Fig. 13). Our goal in this study has been to identify and map the dolomitization distribution within the anticline.

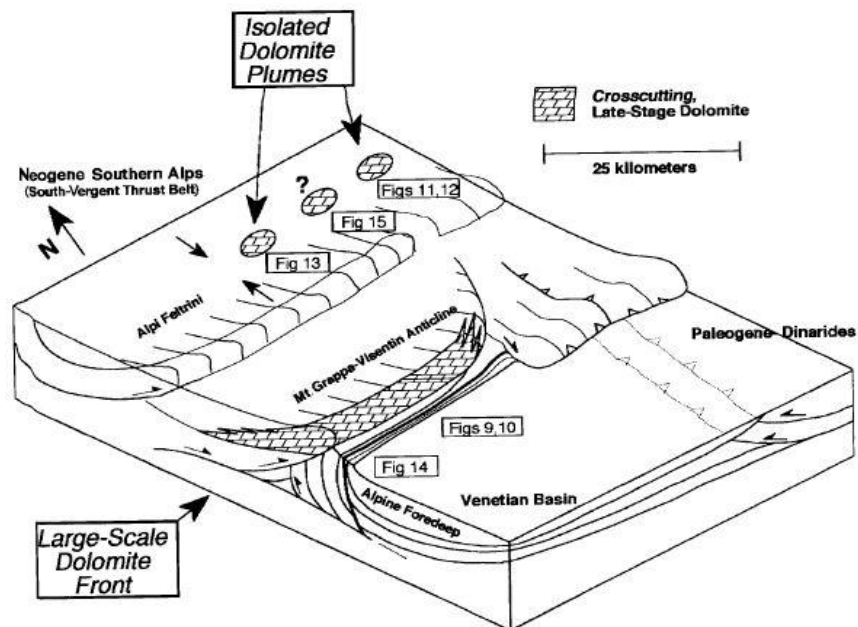


**Fig 13:** From Zempolich & Hardie, 1997. Conceptual model of distribution of the dolomite bodies along fault zones. The fluids are rising along the stratigraphic succession using the faults as preferential ways.

Between the Oligocene and Miocene, during the Neo-Alpine compression phase, tectonic loading increased the pressure of the pore fluids and made them migrate through sediments rich in Mg (dolostone), using faults as preferential ways (Fig. 13). Pore fluids became thus enriched in Mg and are thought to have caused the diffuse dolomitization observed in many portions of the Venetian prealps (e.g., Zempolich & Hardie, 1997; Ronchi et al., 2012; Di Cuia et al., 2014).

The link between tectonics and dolomitization is evident also in other alpine tectonic structures in the Venetian Southern Alps, as the M. Grappa fold (Ronchi et al., 2012) and in the Asiago plateau (Di Cuia et al., 2014). The dolomitization in our study area has been attributed to a mechanism similar to the squeegee model (Ronchi et al., 2012). According to the squeegee model, the fluids were squeezed from the Alpine main thrusts southwards towards the foreland basin.

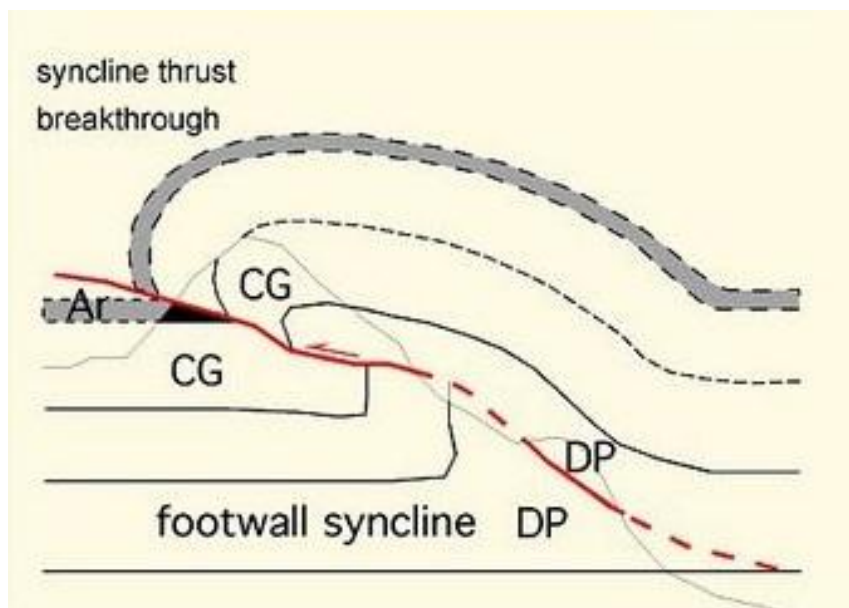


**Fig14:** Picture modified from Doglioni, 1992. It's a representation of a once thrust that cut an anticline at the base, providing to the fluids a preferential pathway.

## **2 Material and methods**

For this project of thesis two different softwares have been used: ArcGIS and Skua-Gocad.

ArcGIS:

ArcGIS is a geographic information system(GIS) for working with maps and geographic information. The ArcGIS is one of the most used softwares for the construction and representation of topographic and geological data. It is used for creating and using maps, compiling geographic data, analyzing mapped and discovering information. The data collected at the end of the survey, have been used by ArcGIS software to produce the geological map.

Skua-Gocad:

In the last years the 3D geological modelling has been used in hydrocarbon exploration for the characterization of the reservoirs, and Skua-Goad is one of the softwares used to build the models. In particular, the main goal for which it is applied is the realization of flow simulations and distribution of petro-physical properties. The information that can be obtained is essential in the analysis of the possible reservoirs production scenarios (Skua 2015 User Guide).

To understand the work done with the Skua-Gocad software, a short explanation of the different phases of work is necessary. The 3D modelling goes through these following steps of work.

1°Modeling of the geological surfaces that define the object of the investigation (in my case for this work the objects are geological boundaries between formations, faults and sections.

2°Building of the volumes defined from the modelled geological surfaces. In the discretization of the volumes they are transformed into grids of squared cells.

3° Distribution of the different petro-physical properties into the grids, through the attribution of values to the grid's cells. This process is facilitated by using different geostatistical techniques. In the case of this thesis, a Kriging method was applied. The difference between Skua-Gocad and other 3D modeling softwares (e.g., Petrel) is essentially the different way of building the cell volume and the distribution of the properties into the created volume.

This work was subdivided in three main parts:

1. Data collection (geological mapping in the field)
2. Digitization on the geological map, in ArcGIS.
3. 3D modeling of the geological structure and dolomitization front with Skua-Gocad.

### **3 Data Collection**

The survey area is located between the Treviso and the Belluno provinces. Previous geological maps at the scale of 1:10.000 existed for the Treviso Province (Bondesan et al., 2011), while for the area of the Belluno Province no geological maps were available at the required scale.

The CTR topographic map of the Veneto region was chosen as a topographic base (downloaded from <https://www.regione.veneto.it/web/ambiente-e-territorio/carta-tecnica-regionale>). In the field, the mapping was performed by annotating outcrops on the topographic map and on a portable GPS device. Layering attitudes and the orientations of the geological structures (faults and folds) were collected with a magnetic compass.

The geologic survey started in September and was finished at the beginning of December 2017. During the survey, 280 gps points were collected (Fig.15), 110 of which are records of the dolomitization front, 15 were collected along faults and breccia deposits, while 250 points represent bed attributes. For the Belluno area, only one old geological map (F. 063 Belluno, 1996, 1:50.000). The survey was carried out with particular attention to the detection of the dolomitized areas, since the principal aim of this work was the reconstruction of the dolomitization front on the significant portion of the Col Visentin - Monte Garda anticline.

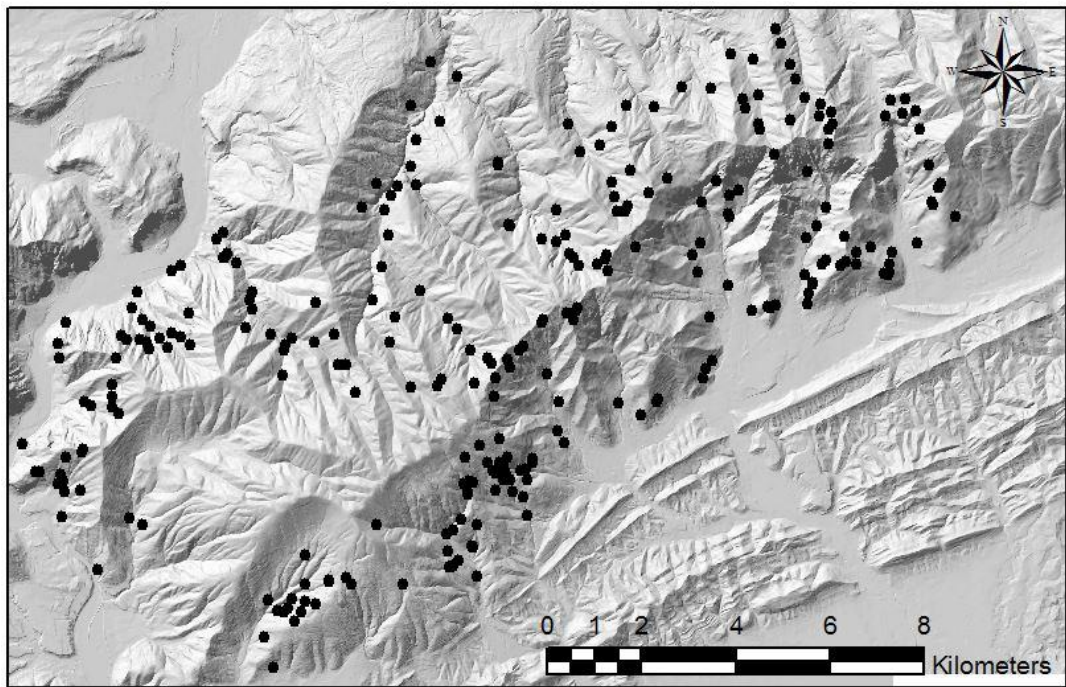


**Fig 15:** The DTM of the study area with the collected GPS points

## 4 Geological map and description

The geological map (Fig. 16) covers an area of 300 km<sup>2</sup>. The mapped lithostratigraphic units are the Igne Formation, the Vajont Oolitic Limestone, the Fonzaso Formation, the Maiolica and the Scaglia Variegata Alpina. Beneath the Igne Formation lies the Soverzene Formation, which however was not found in the area of survey.

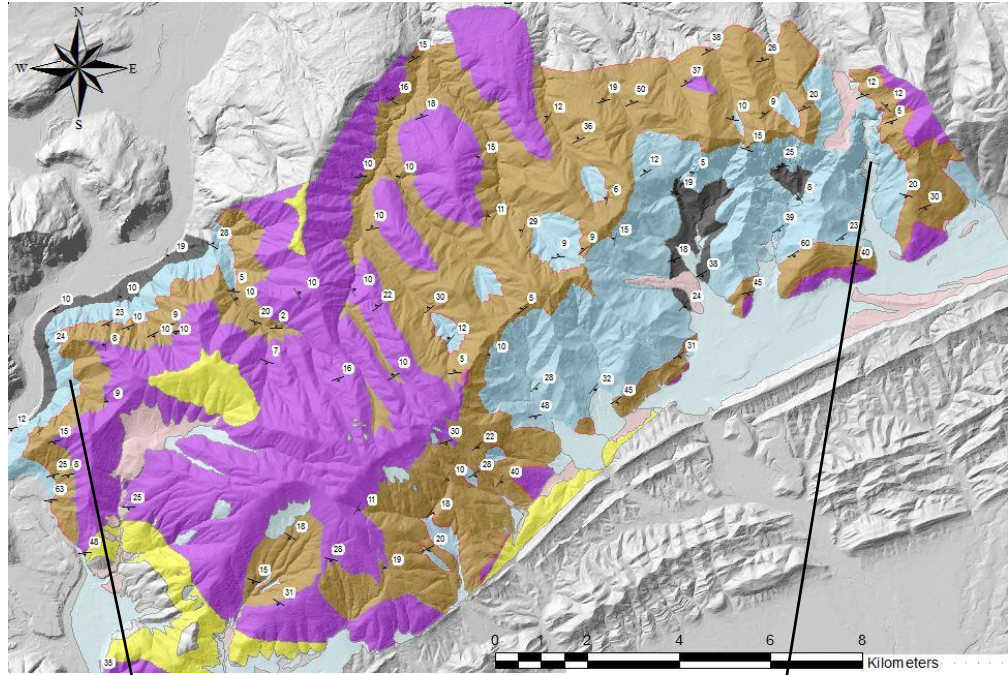
The Igne Formation has a constant thickness of 150 m - 200 m, it was found in just two portions of the mapped area, near Praderadego, and in the Quero Valley. The Vajont Oolitic Limestone changes its thickness from East to West. In the Eastern portion of the area of interest, near San Boldo Pass, the Vajont Oolitic Limestone has been completely dolomitized, and its thickness is around 390 m, while it reaches less than 270 m along the Quero Valley.

The Fonzaso Formation maintains its thickness constant along the whole area, about 350 m - 380 m. As far as the structure is concerned, the geological map shows two fault systems crosscutting the Jurassic sequence with N° - S° and NE° - SW° trends respectively.

The N° - S° faults extend especially on the west side of the study area and define the main tectonic structure of the Col Visentin-Monte Garda anticline. Probably these faults represent a reactivation of old Mesozoic lineaments. The NE° - NW° faults are recognized in the whole area.

They are small faults that didn't cause remarkable dislocations.





stratigraphic log of Quero- Vas					
NOTES	FORMATION	AGE	SCALE (m)	LITHOLOGY	STRUCTURES / FOSSILS
nodular limestone, silt - clay	scaglia	Serravallian	14	[stippled pattern]	[fossil symbols]
			13	[stippled pattern]	
pelagic mudstone with chert	Maolica	Tithonian	12	[brick pattern]	[fossil symbols]
			11	[brick pattern]	
marl - silt	Fonzaio	Callovian-Kimmeridgian	10	[brick pattern]	[fossil symbols]
			9	[brick pattern]	
bio-clastic limestone	Vajont	Ordovician	8	[brick pattern]	[fossil symbols]
			7	[brick pattern]	
Oolite Grainstone-Packstone	Vajont	Ordovician	6	[brick pattern]	[fossil symbols]
			5	[brick pattern]	
marly - limestone	Igne	Aalenian	4	[brick pattern]	[fossil symbols]
			3	[brick pattern]	
org. matter bituminous dolostone	Soverzene	Toarcian	2	[brick pattern]	[fossil symbols]
			1	[brick pattern]	

Stratigraphic log of San Boldo Pass					
NOTES	FORMATION	AGE	SCALE (m)	LITHOLOGY	STRUCTURES / FOSSILS
nodular limestone, silt - clay	scaglia	Serravallian	15	[stippled pattern]	[fossil symbols]
			14	[stippled pattern]	
pelagic mudstone with chert	Maolica	Tithonian	13	[brick pattern]	[fossil symbols]
			12	[brick pattern]	
marl - silt	Fonzaio	Callovian-Kimmeridgian	11	[brick pattern]	[fossil symbols]
			10	[brick pattern]	
bioclastic limestone	Vajont	Ordovician	9	[brick pattern]	[fossil symbols]
			8	[brick pattern]	
Oolite Grainstone-Packstone	Vajont	Ordovician	7	[brick pattern]	[fossil symbols]
			6	[brick pattern]	
marly - limestone	Igne	Aalenian	5	[brick pattern]	[fossil symbols]
			4	[brick pattern]	
org. matter bituminous dolostone	Soverzene	Toarcian	3	[brick pattern]	[fossil symbols]
			2	[brick pattern]	
			1	[brick pattern]	

**Fig 16:** Geological map of the Col Visentin – Monte Garda anticline, with two stratigraphic logs showing the thickness variation of the Vajont Oolitic Limestone.

## **4.1 Improvements of the geological map**

The new survey of this thesis (Fig. 17, 18) allowed an improvement of the geological map of Bondesan et al. (2011). The greatest differences have been introduced in the area between San Boldo Pass and Praderadego, where the boundary between the Vajont Oolitic Limestone and the Fonzaso Formation has been significantly lowered.

Along the Cison di Valmarino and Praderadego valleys the outcrop area of the Igne Formation has been broadened. The most important improvement however, was the new mapping of a large portion of the anticline that, being outside of the Treviso province, was not considered in Bondesan et al. (2011).

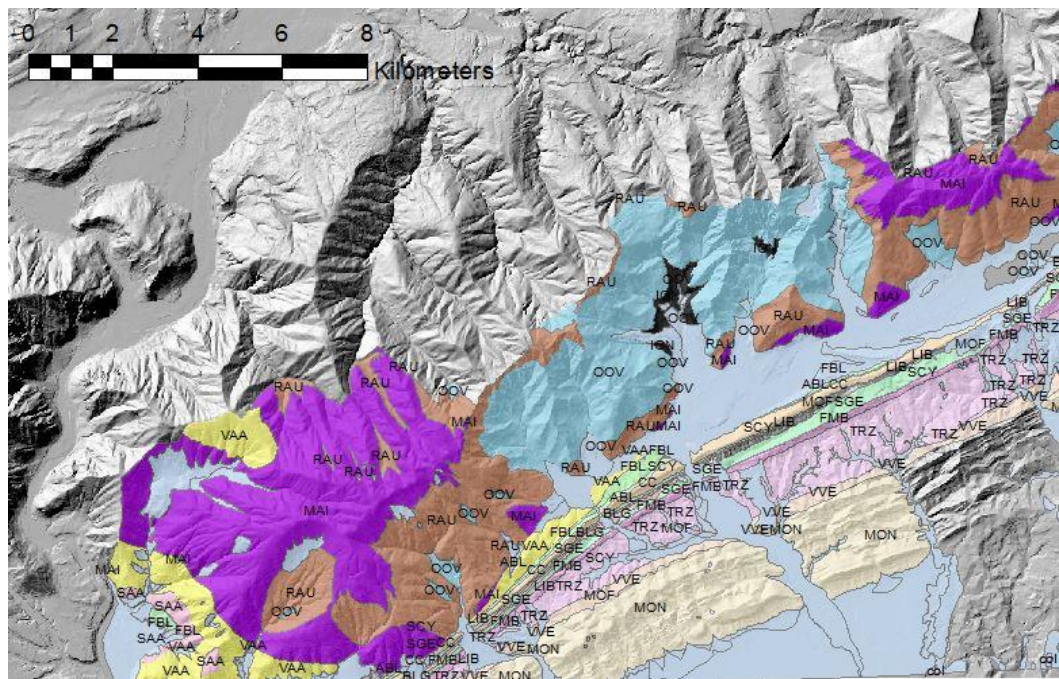


**Fig 17:**A rendering of the geological map by Bondesan et al. (2011), which ends at the border between the Treviso and Belluno provinces.

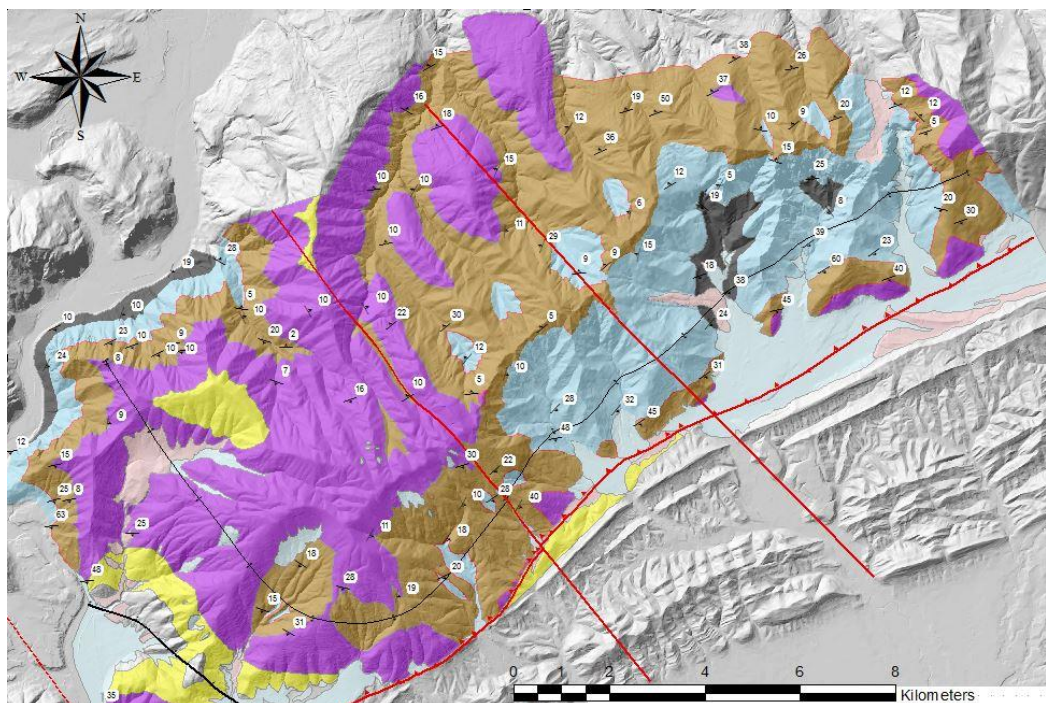


**Fig 18:** The improved geological map of the Col Visentin – Monte Garda anticline

## 4.2 The Col Visentin - Monte Garda anticline

The whole study area is situated on a knee anticline structure, which has a ENE° - WSW° trend. This anticline structure is nearly cylindrical in the eastern part from San Boldo Pass to Combai, but its strike changes from NE° - SW° to NW° - SE° in the western part of the study area (see figure 19). The anticline formed during Neo-Alpine compression, which began in the Oligocene. The change in strike direction near Segusino has been related to the Quero strike slip fault, that has been active during the Serravallian to Messinian.

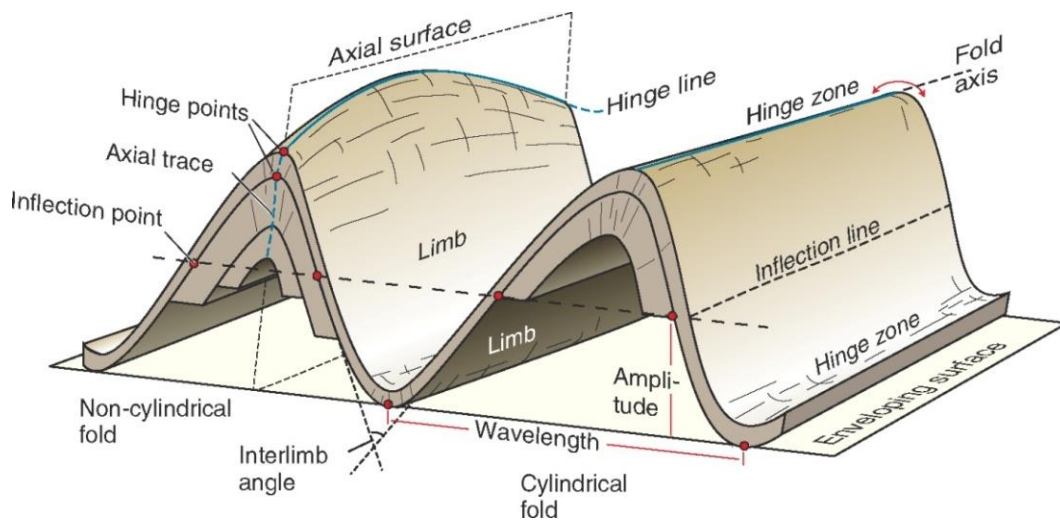


**Fig 19:** Differences between a cylindrical and a non-cylindrical fold, (picture from Sanuja Senanayake)

During the survey, the geological information (dip, azimuth, strike) was collected, from the parasitic folds especially developed into the Scaglia Variegata Alpina and the Maiolica and in some cases into deeply deformed areas of Fonzaso Formation.

These parasitic folds have a small wavelength and amplitude. They can show a typical S or Z asymmetric profile (Fig. 20), and M profiles in the hinge regions of the Col Visenin – Monte Garda anticline.



**Fig 20:** Picture taken on the N 143 provincial road near Valdobbiadene, shows a spectacular parasitic folds, type Z, into the Scaglia Variegata Alpina, highlighted by the black lines.

Variations in the linearity of the anticline hinge were detected. There are two great examples where this variation is fully visible (Fig. 21).

On the top of Praderadego valley the Col Visentin - Monte Garda anticline shows a culmination that encloses a large area of the Eastern part of the anticline (Fig 15). The elevation of the structure is understandable by the presence of the Igne Formation at the base of the valley, while only a small thickness of this formation is present in the nearby valley of Cison di Valmarino.

Between Valdobbiadene and Segusino, a progressive sinking of the anticline hinge defines a hinge depression.

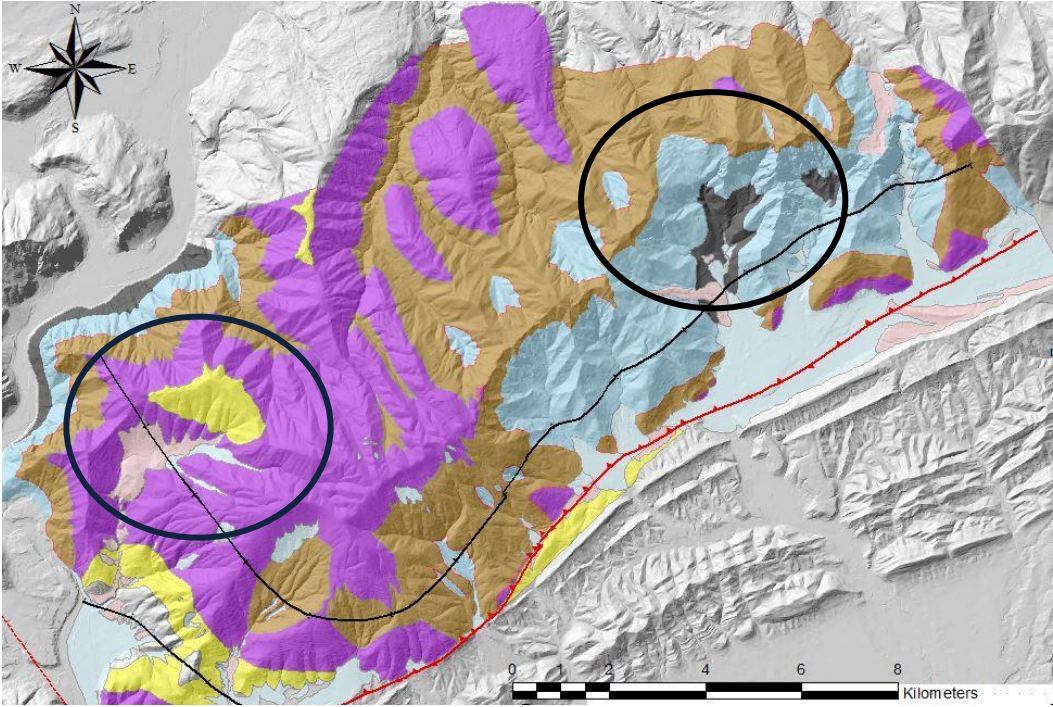


**Fig 21:** Simplified geological map of the study area. The black circle encloses a culmination of the fold hinge while the blue circle encloses the main hinge depression. The black line represents the position of the anticline hinge line.

### 4.3 Mapping of the dolomitized area

A particular attention was also paid to the mapping of the dolomitized bodies. Field data about the dolomitization, were already available from Bondesan et al. (2011). The newly done geological survey of this work significantly improved the mapping of the dolomitization front (Fig. 22). The Vajont Oolitic Limestone is dolomitized for all its thickness, except for the area of Praderadego. A partial dolomitization of the above and underlying formations is often observed. The total thickness of the dolomite body along the Col Visentin - Monte Garda may exceed 500-600 m and dolomitization of the underlying Igne Formation and Soverzene formation has occurred.

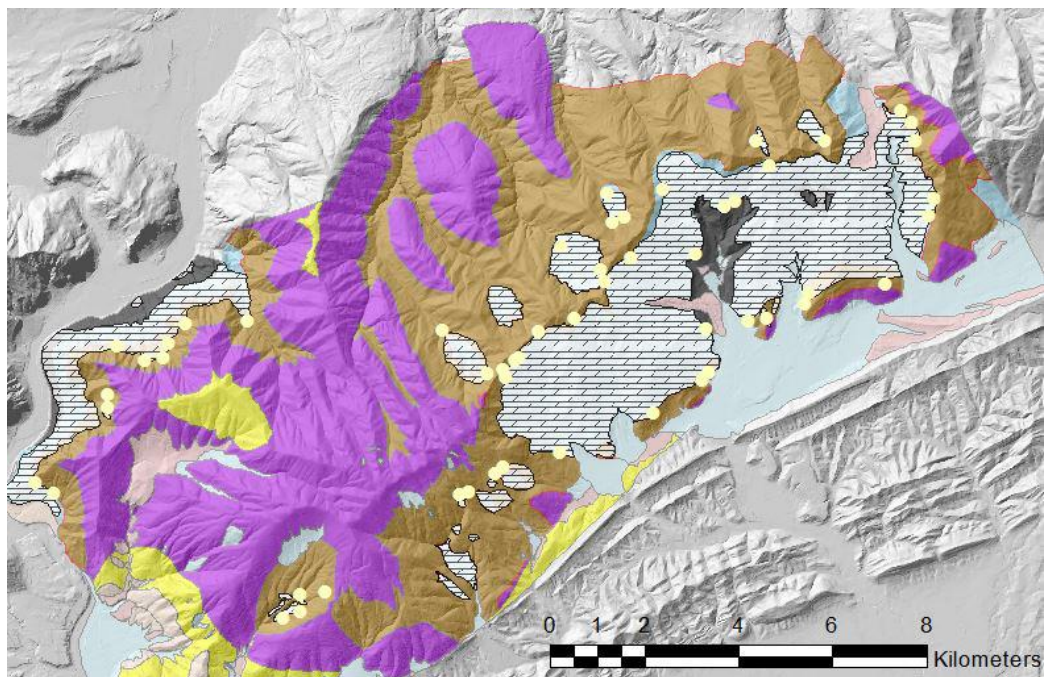


**Fig 22:** Geological map of the whole area of study, where the dolomitization is represented by the dashed white blocks, the light yellow points are the top dolomitization GPS points.

The field work was focused on the mapping of the dolomitization front, the stratigraphic position of the dolomitization with respect to the top of the Vajont Oolitic Limestone was recorded wherever possible. Along the hinge, the highest dolomitized portions were found near or along faults, cutting the Fonzaso Formation. Along these faults the dolomitization extended in the surrounding rocks for 10-20 m. In some areas as Cison di Valmarino, Tovenà and Quero, the dolomitization was identified into breccias in contact with the Maiolica Formation, while along some faults of the same area the dolomitization stopped much lower.

The dolomitization of the Vajont Oolitic Limestone in the study area has been interpreted as a case of squeegee dolomitization related to the Neo-Alpine tectonic phase by Zempolich & Hardie (1997). A similar process has been documented by Di Cuià et al., (2011) in the Asiago plateau and by Ronchi et al., (2012) at the Monte Grappa. In these two cases the Vajont Oolitic Limestone is not present and the dolomitization affected a carbonate platform succession of the Calcari Grigi Group, early Jurassic age. Nevertheless the fault zones were preferentially dolomitized in these cases as well. According to both Di Cuià et al., (2011) and Ronchi et al., (2012) dolomitizing fluids were injected into the faults when they were still active during Alpine compressional phases. It is also plausible that the dolomitization of the Vajont Oolitic Limestone was possible because the oolites retained some primary porosity, and consequently dolomitizing fluids could spread from faults into the whole thickness of the Vajont Oolitic Limestone.

The origin of massively replaced dolomite has remained one of the major unresolved problems of the sedimentology and sedimentary geochemistry. In the eastern part of the Southern Alps, during the Alpine deformation, convection driven fluids derived from Late Tertiary seawater were circulated through subaqueous Alpine-aged faults and fractures and paleosedimentary breccias, thus creating the different dolomite bodies found in the Vajont Oolitic Limestone and others Mesozoic basal sediments. The connection between the dolomite bodies and the Alpine compressional phase suggests that the dolomitization was a



late and high-temperature process, and that it was active during the Alpine compression or post compression, following the squeegee model (Zempolich & Hardie, 1997; Ronchi et al., 2012).

The dolomitization front has been mapped below the contact between the Vajont Oolitic Limestone and the Fonzaso Formation only in the area of Praderadego (Fig. 24). This zone is a culmination of the hinge of the Col Visentin – Monte Garda anticline. The dolomitization on the limbs of the Anticline reaches well above the top of the Vajont Oolitic Limestone (see figure 23).

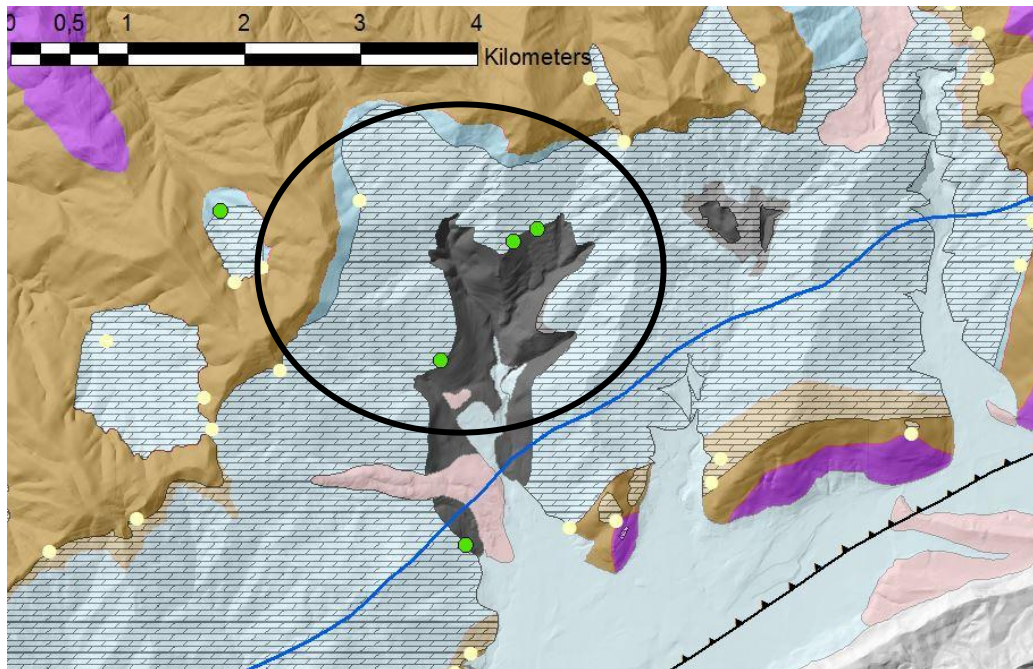


**Fig 23:** Large scale view of the top dolomitization in the area of Praderadego. The culmination area is enclosed in the black circle. The yellow points are the top dolomitization and the green dots represent the base of the dolomitization

## 5 Topographic model

The data used for the realization of the 3D model of the Col Visentin - Monte Garda anticline are surface data, derived from field mapping.

In order to prepare the topographic base for the 3D model, the airborne Lidar point cloud acquired by the Treviso Province, and the DTM of the Belluno Province, were merged to cover the entire study area. Data can be downloaded free from (<https://www.regione.veneto.it/web/ambiente-e-territorio/geoportale>).

Every block of the Belluno DTM is formed by approximately 3 million points, which added to the point cloud of Treviso, makes 20 million points. This amount of data was too heavy to the workstation to be used for the modelling, hence the point cloud was decimated by using Cloud Compare to form a unique point cloud made of 1 million points (Fig. 24). The working mesh surface was produced in Skua-Gocad (Fig 25).

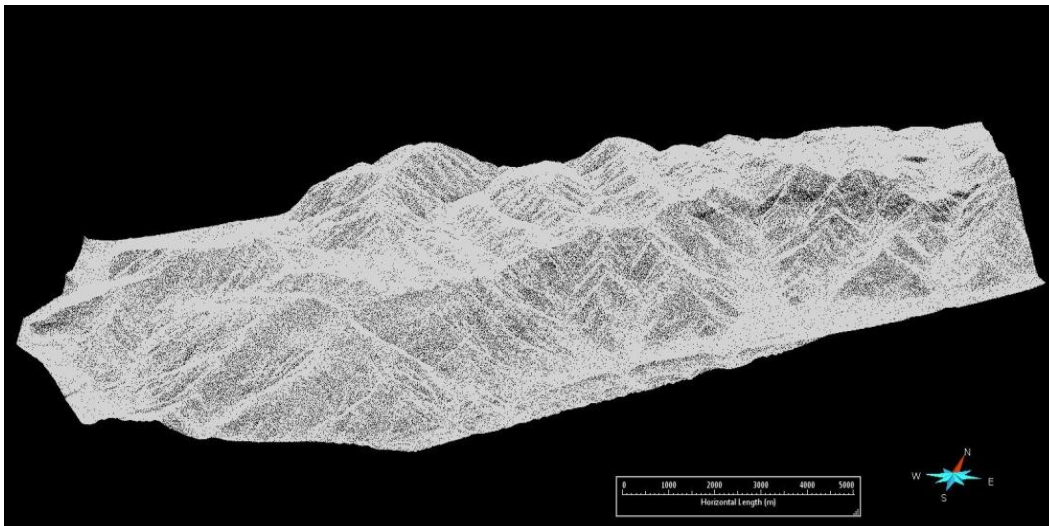


**Fig 24:** Points cloud of the topographic base of the study area, composed by 1 million points (snapshot from SkuaGocad).

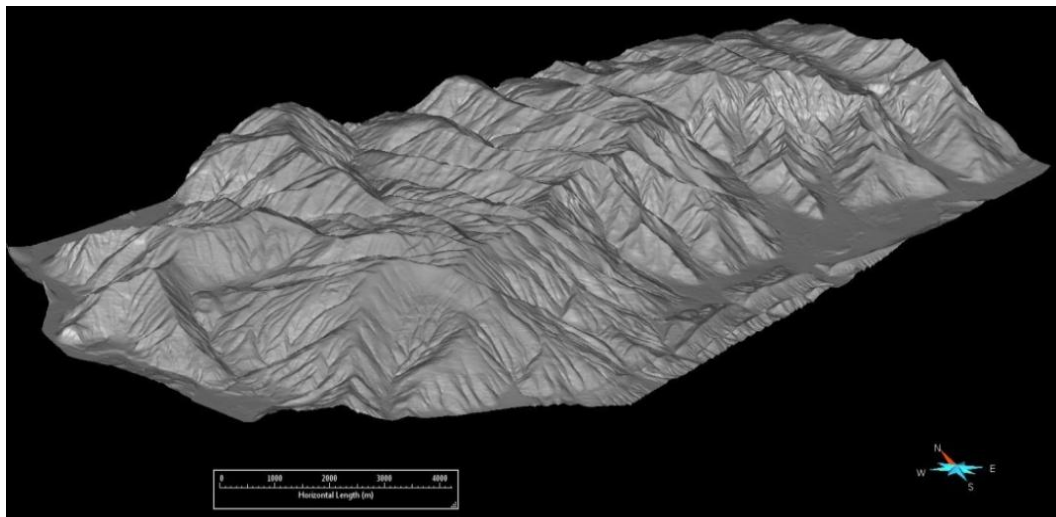


**Fig 25:** The mesh created by the interpolation of 1 million points, with 5 meters of vertical accuracy.

## 5.1 Geological modeling with SkuaGocad

To realize the 3D model tree main steps were taken in SkuaGocad.

In a first step, a structural model was built including the geological boundaries (Fig. 26) and faults that were surveyed on the area of interest. In this step, different kinds of data were imported: faults, boundaries between formations, gps points with attached geological information (e.g., bed altitude, dolomitization, litology) and drawn cross sections. In a second step, the geological grid was generated using the Structural and Stratigraphy workflow. In the third step the Gaussian curvature of a chosen geological surface - namely, the boundary between the Vajont Oolitic Limestone and the Fonzaso Formation was calculated

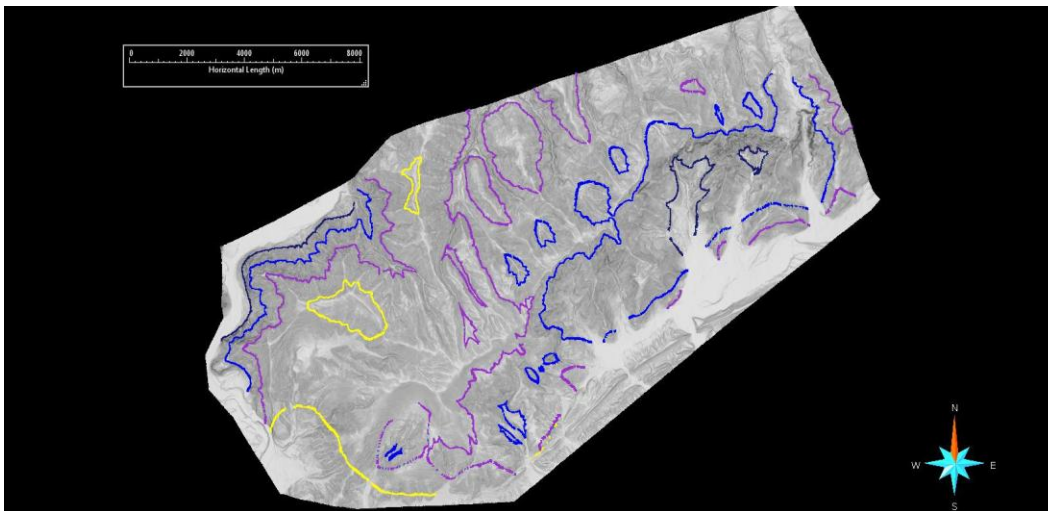


**Fig 26:** Boundaries between formations, projected on the mesh. The dark-green line is the upper Igne Formation, the blue line is the upper boundary of the Vajont Oolitic Limestone, the pink line is the upper boundary of the Fonzaso Formation, the yellow line is the upper boundary of the Maiolica.

### 5.1.1 Geological cross sections

For the 3D representation of the geological model, in addition to the surface data projected on the create surface (fig. 27), 13 cross sections were realized that cut the whole complex structure.

The positions of the cross sections on the area were chosen to allow the best depiction of the whole structure. In the western part of the structure, close to Valdobbiadene, due to the greatest complexity of the fold, the cross-sections are denser.

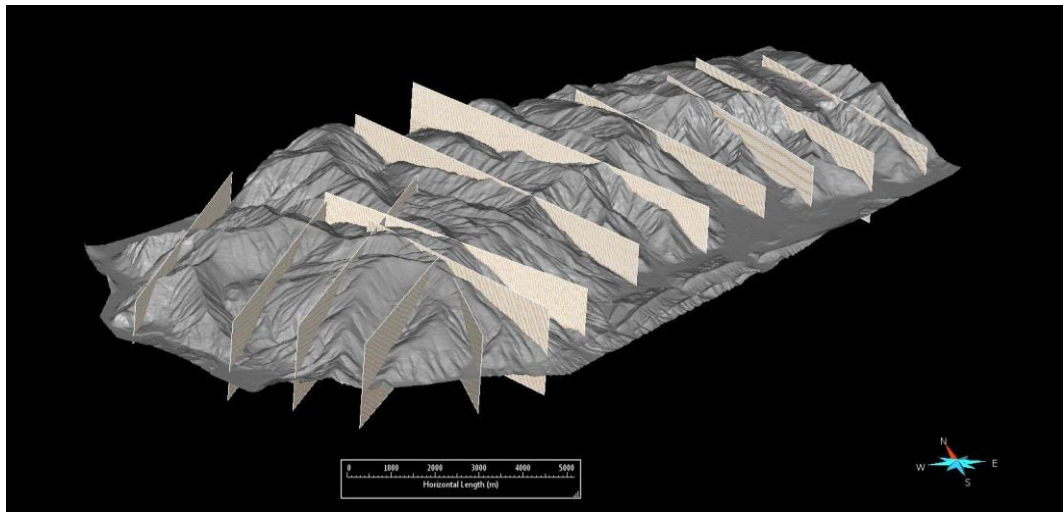


**Fig 27:** The mesh surface with the thirteen drawn cross sections intersected to the triangulated surface.

### 5.1.2 Generation of boundary surfaces

Three surfaces, corresponding to formation boundaries, were built with SkuaGocad at the base the Igne Formation, at the Igne/Vajont boundary, and at the Vajont/Fonzaso boundary and the boundary between Fonzaso/Maiolica on the top. The sections were drawn and then they were uploaded on SkuaGocad as voxets. The cross sections, were used to further constrain the boundaries between formations in the subsurface (Fig. 28).

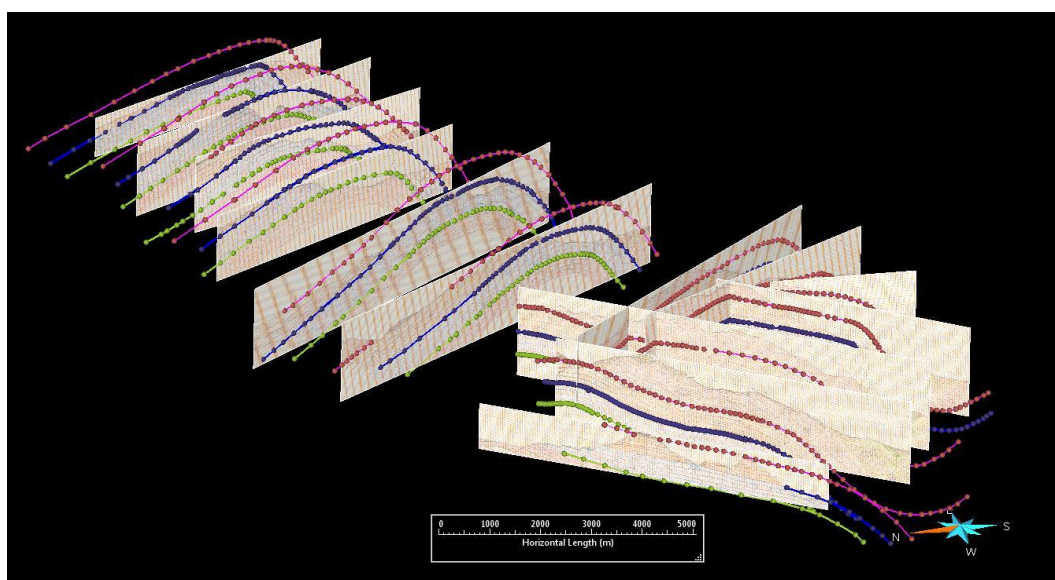


**Fig 28:** All the cross sections inserted into the project, and the digitized formation boundaries. The pink polylines represent the Fonzaso Formation-Maiolica boundary, the blue polylines represent the Fonzaso Formation-Vajont Oolitic Limestone boundary and the light green polylines represent the Vajont Oolitic Limestone-Igne Formation boundary.

The obtained horizons show thickness variations in some cases, especially in the limbs zones of the anticline structure.

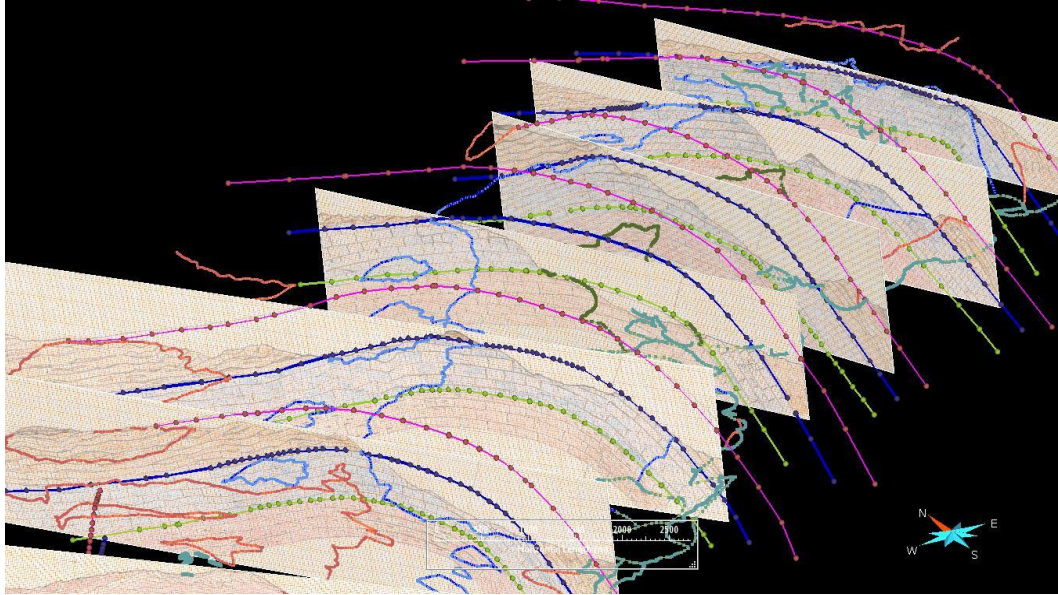


**Fig 29:** The boundaries traced along the cross sections, fitting the boundaries projected on the mesh surface.

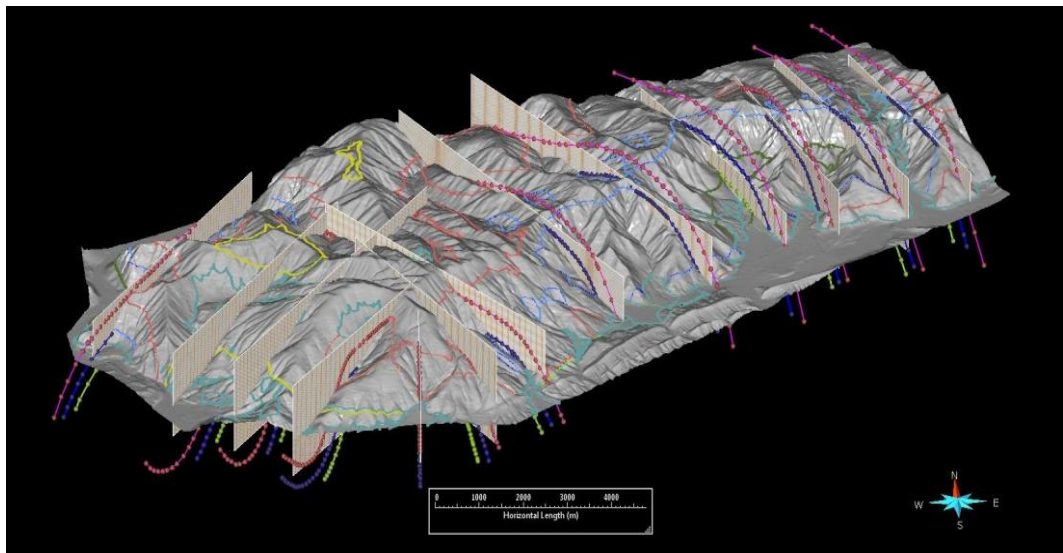


**Fig 30:** The digitized formation boundaries from cross sections and field survey, overlapped to the triangulated topographical mesh

The surfaces corresponding to formational boundaries were then built with the horizons building processing with the Structural and Stratigraphy workflow by Skua-Gocad.

This process allows the building of every horizon surface at the same time, which facilitates the build-up of a structurally coherent model.

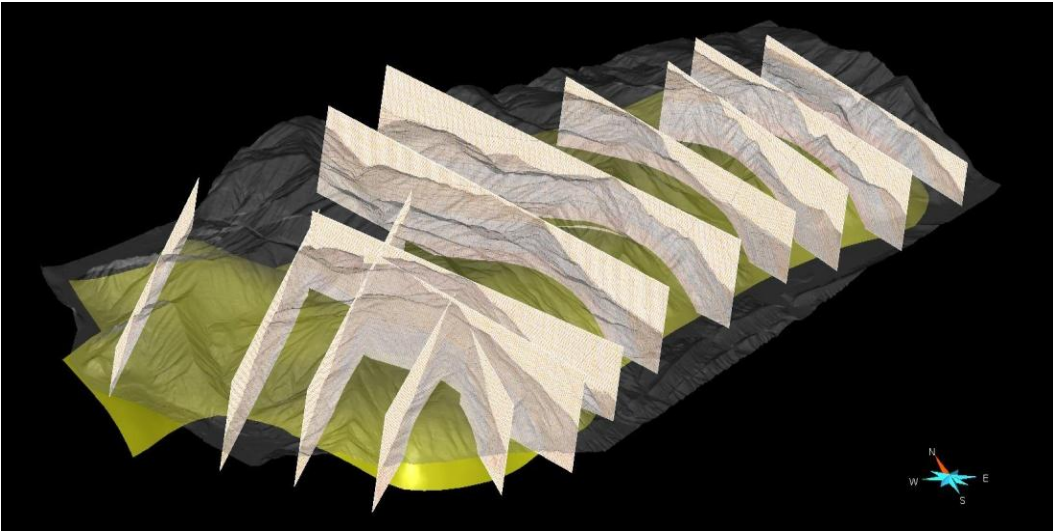


**Fig 31:** The base of the Igne Formation

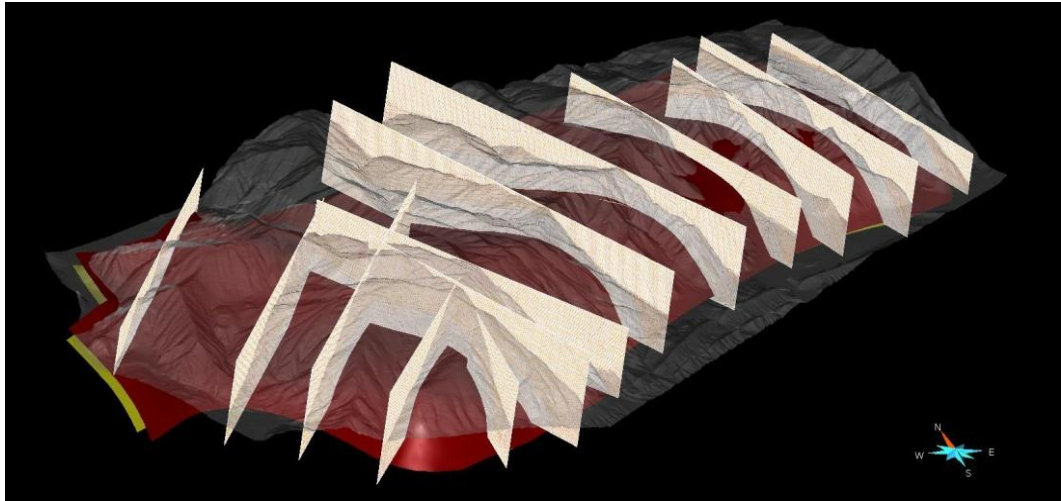


**Fig 32:** The top of the Igne Formation



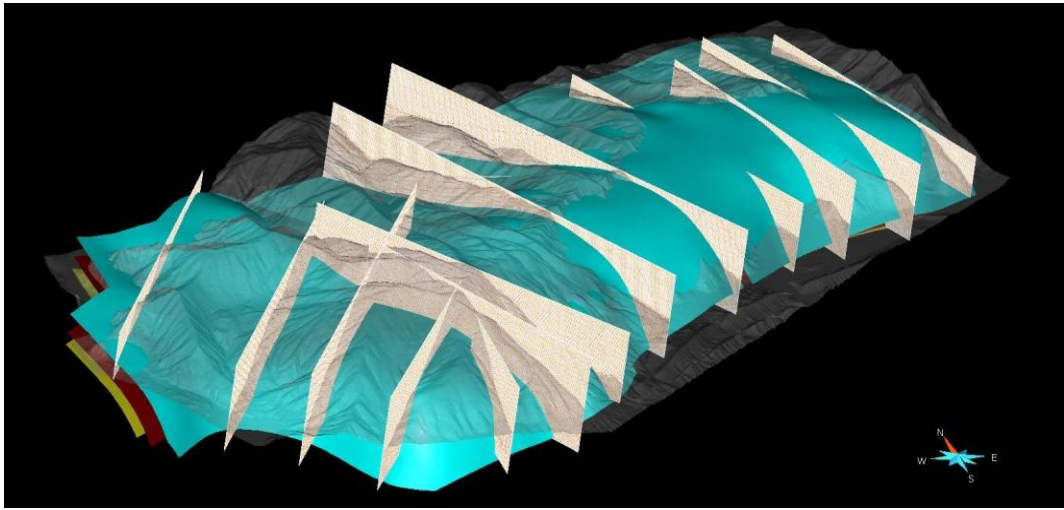


**Fig 33:** Top of the Vajont Oolitic Limestone

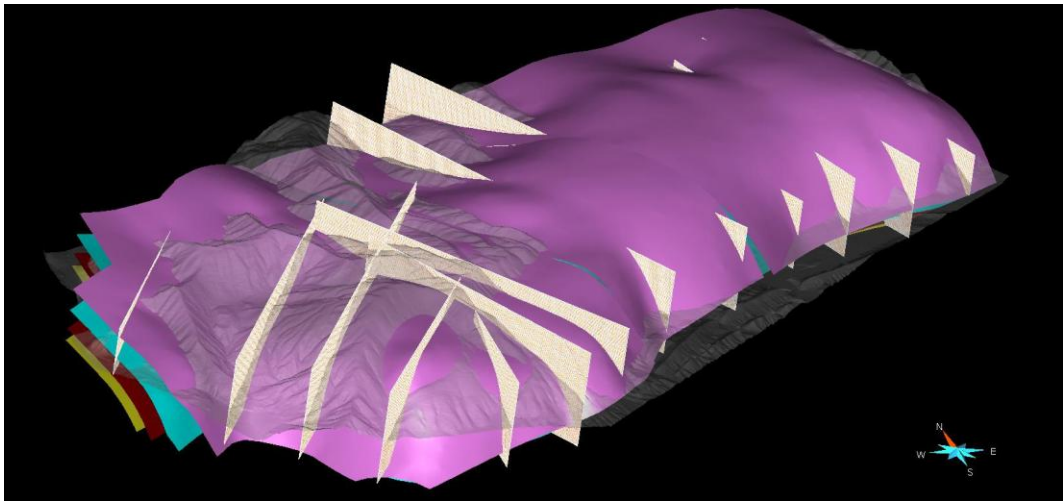


**Fig 34:** The top of the Fonzaso Formation

After the horizons building process generated the formational boundaries surfaces, these can be adjusted to better fit the available data. During this process the dataset was filtered in order to exclude a part of the dataset that may include some inconsistencies in the horizons, a low degree of smoothing was used, to obtain the maximum fitting of the available data.

The geologic surfaces fitting the digitized polylines were reconstructed in 3D as triangular meshes using the horizon building process in the Structural and Stratigraphy Workflow (Fig. 35). At the end of this process, when the surface for each of the boundaries was done, it was possible to proceed with the creation of a gridded volume.

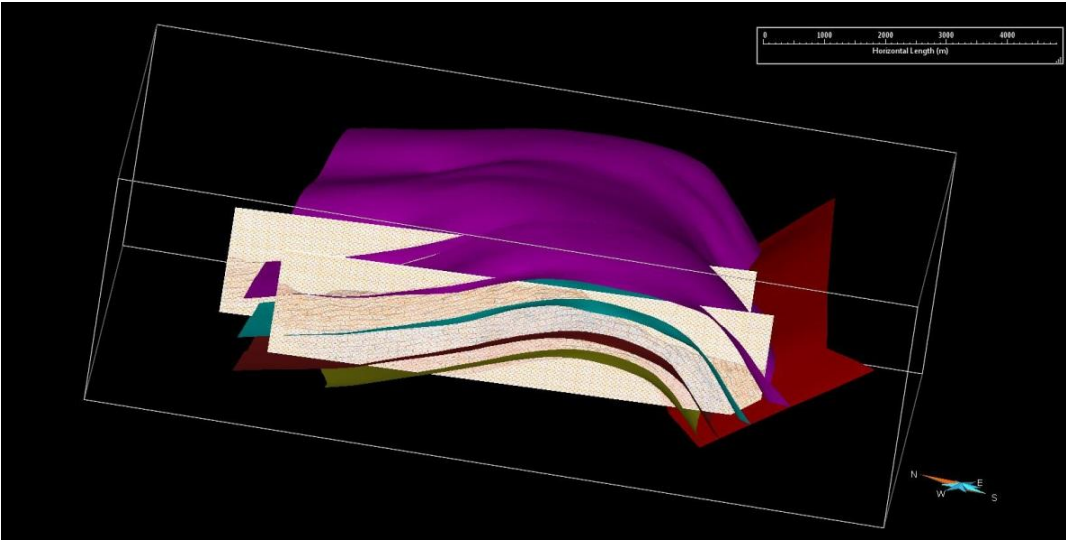


**Fig 35:** A detail of the anticline eastern portion, the realized horizons fit the drawn sections boundaries.

### 5.1.3 The geologic grid of the anticline structure

The production of a geological grid of the Col Visentin - Monte Garda anticline was the last step of the Structural and Stratigraphy Workflow.

The geological grid was realized considering a Volume of Interest (VOI-BOX) that comprises only the relevant objects of the model. It was refined by many attempts. Our VOI extends from -950 m below sea level to 1900 m above sea level (Fig. 36).

The fault network was created using the Follina and Combai faults and the Bassano - Valdobbiadene thrust, while other supposed lineaments (blind back thrust and the fault in the western portion of the structure) were not used.

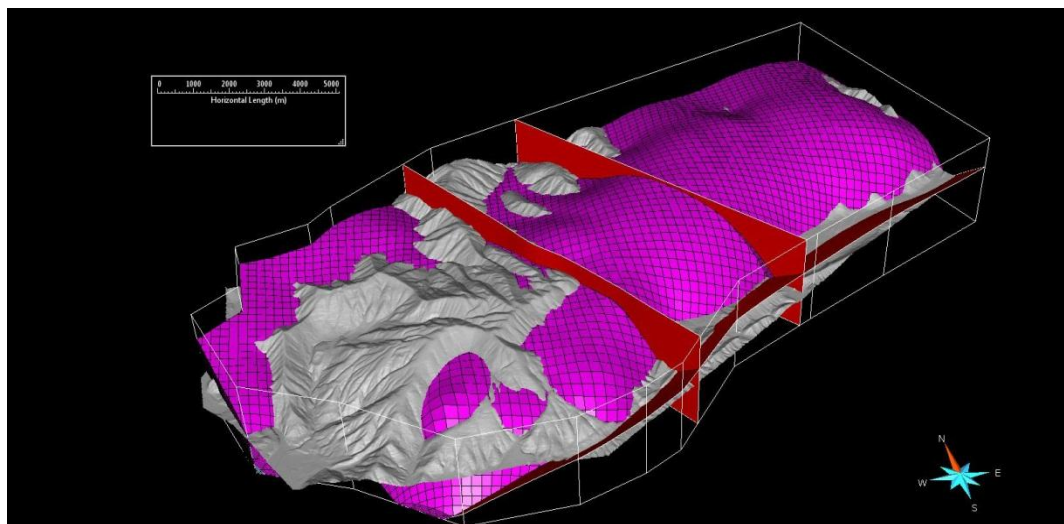


**Fig 36:** The geological grid with the faults network red surfaces, within the VOI-BOX

The volume for each formation is defined by faults and horizons and is separate into cells of user-defined size. The faults were edited and extended to the boundaries of the VOI.

The areal cell size of the grid was chosen to be 200 m x 200 m, and 10 cells were created in the vertical direction for each stratigraphic unit (Fig. 37).

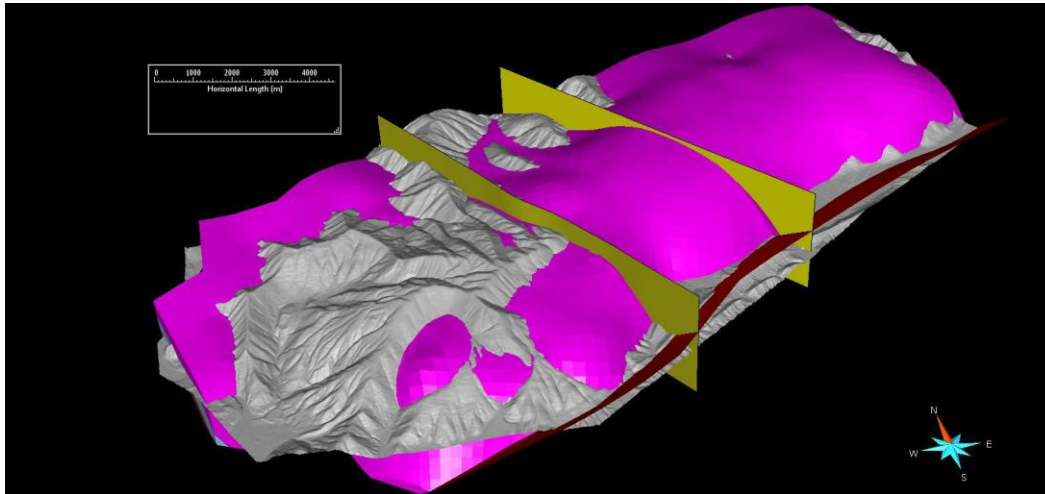


**Fig 37:** The geological grid with Skua-Gocad, red:the Igne Formation, blue: the Vajont Oolitic Limestone, pink: the Fonzaso Formation, are represent also the lineaments, the yellow surface: Follina fault, the brown surface: Combai fault, dark brown surface: Bassano – Valdobbiadene thrust.

Four cross sections were then built in Skua-Gocad, to check the accuracy of the modeled horizons and grid volumes (Fig. 38, 39, 40, 41, 42).

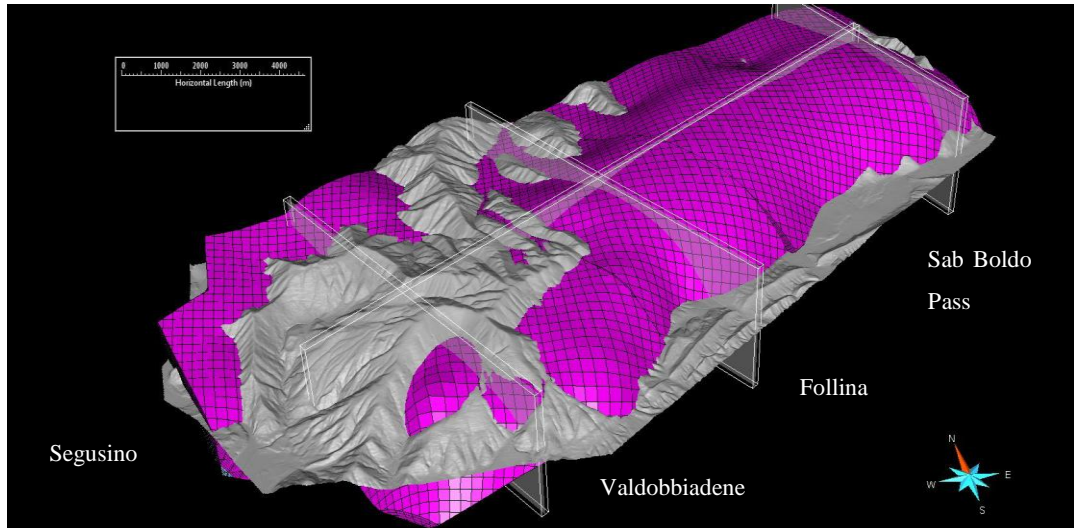


**Fig 38:** Location of the five cross section digitalized by Skua-Gocad

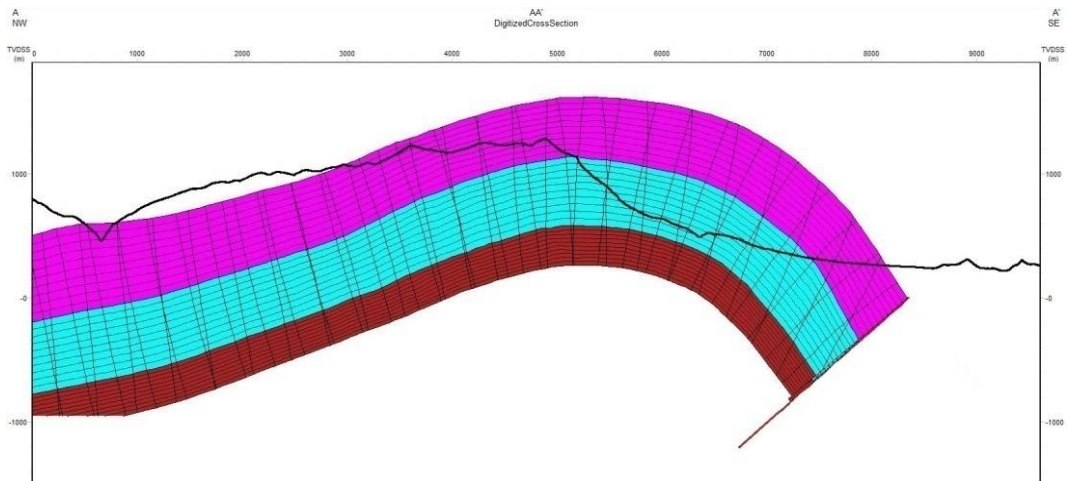


**Fig 39:** The Follina cross section pink:Fonzaso Formation, blue: Vajont Oolitic Limestone, red: Igne Formation, the dark brown to the SE° is the Bassano – Valdobbadiene thrust.

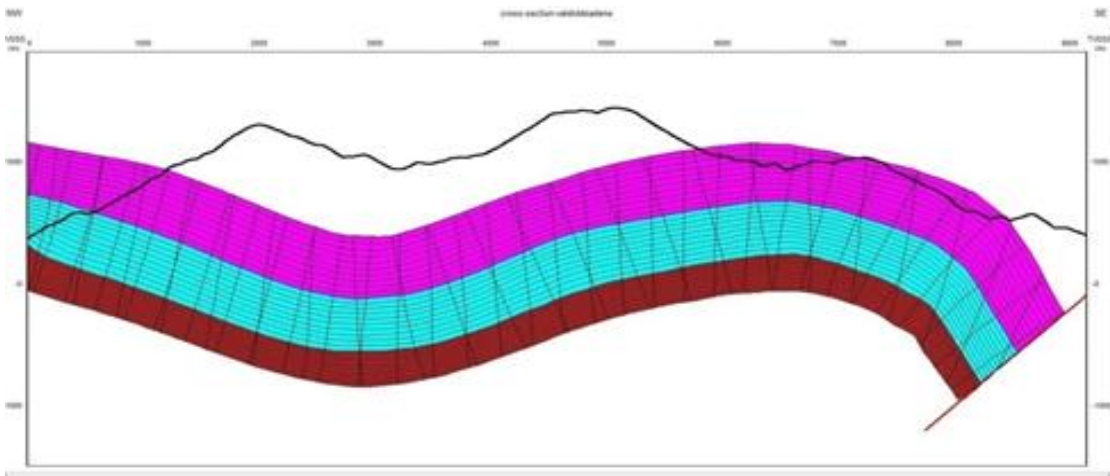


**Fig 40:** The Valdobbiadene cross sections, pink: Fonzaso Formation, blue: Vajont Oolitic Limestone red: Igne Formation, the dark brown surface to SE° is the Bassano-Valdobbiadene thrust.

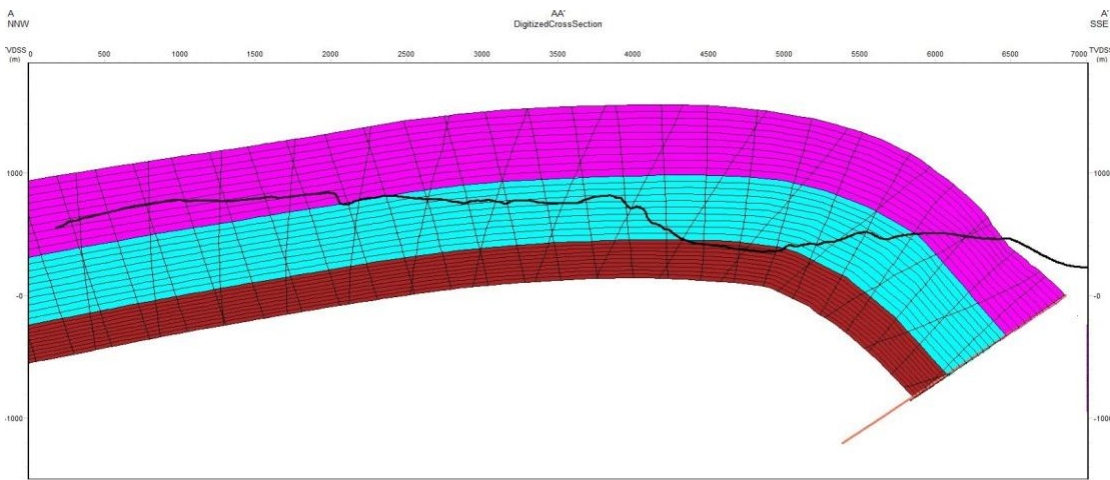


**Fig 41:** The San Boldo pass cross section, pink: Fonzaso Formation, blue: Vajont Oolitic Limestone, red: Igne Formation, the dark brown surface to SE° is the Bassano – Valdobbiadene thrust.

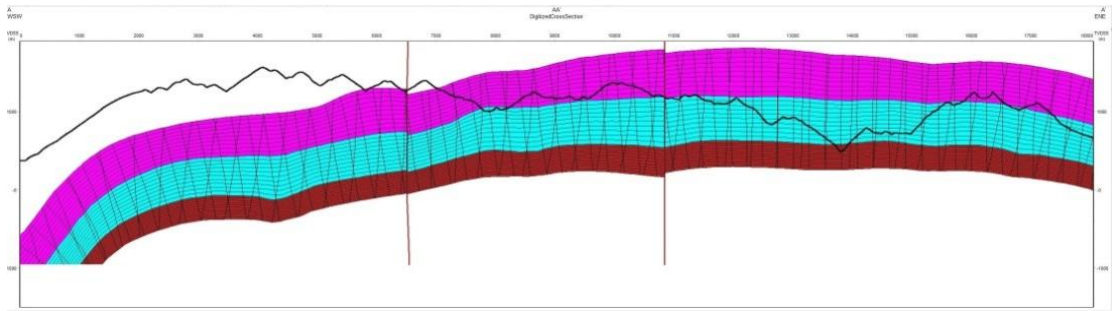


**Fig 42:** The Segusino cross section, pink: Fonzaso Formation, blue: Vajont Oolitic Limestone, red: Igne Formation, the two dark brown line in the middle, are start from East the Combai and the Follina faults.

The modeled volumes (Table 1) of the stratigraphic units within the VOI are as follows:

Grid volumes		
Formation	Thickness	Volume
Igne	200 m	48.377 x 10 <sup>9</sup> m <sup>3</sup>
Vajont Oolitic Limestone	350 m - 400 m	85.936x10 <sup>9</sup> m <sup>3</sup>
Fonzaso	380 m - 430 m	100.197x10 <sup>9</sup> m <sup>3</sup>

**Table 1:** The different grid volumes calculated by SkuaGocad.

### 5.1.4 Features of the Col Visentin - Monte Garda anticline

The 3D model of the Col Visentin - Monte Garda anticline highlights some interesting information about the structural characteristics of this anticline. The Col Visentin - Monte Garda is a strongly asymmetric, south-verging non-cylindrical fold with a ENE° - WSW° trend in its eastern part. Toward the west, a strong change in direction of the axial plane is observed.

Furthermore, the hinge lines exhibit depressions and culminations.

These depressions and culminations are highlighted in figure 43, which shows by a chromatic scale the height variation of the anticline surface, with respect to sea level. This visualization was reached by attribution of the z value (calculated from the zero topographic) for each cell of the grid volume.

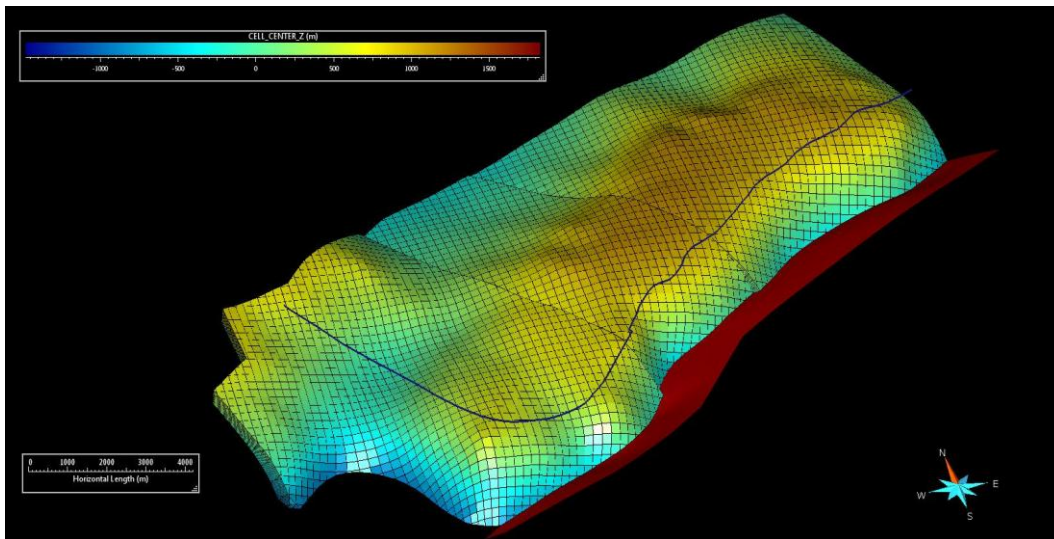


**Fig 43:** Topography of the Col Visentin – Monte Garda anticline, the warm colors correspond the high elevations, cold colors represent a low elevations with respect to M.S.L. The blue line is the axial fold, the red surface is the Bassano – Valdobbiadene thrust



## 5.2 Gaussian curvature

The Gaussian curvature is an intrinsic measurement of the mean curvature depending only distances that are measured on the surface. In non-Euclidean geometry, the Gaussian curvature  $\mathbf{K}$  of a surface at a point is the product of the principal curvatures  $\mathbf{k}_1$  and  $\mathbf{k}_2$  at the given point.

$$\mathbf{K} = \mathbf{k}_1 * \mathbf{k}_2.$$

For example, a point on a cylinder has a zero value of the Gaussian curvature, because the curvature along the cylinder axis is zero. Otherwise, any point on a sphere has a positive the Gaussian curvature.

A common application of curvature analysis is to predict the location and the amount of deformation on the curved surfaces. It is predicted that the areas with a high absolute value of Gaussian curvature may have high fracture density. Some authors have found a relationship between permeability derived from fractures and the calculated curvature (Murray 1968). According to this relationships, the zone of the Col Visentin - Monte Garda anticline that shows highest values of the Gaussian curvature could be more fractured compared to the others zone within VOI.

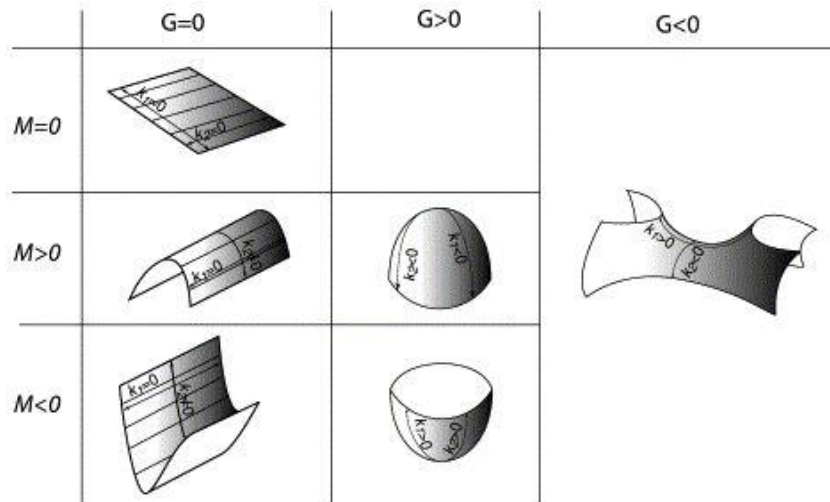


**Fig 44:** The Gaussian Curvature  $G$  is used to infer the shape of the surface **a)**  $G>0$  it is positive at on basins and domes **b)**  $G<0$  it is negative at saddle points **c)**  $G=0$  it is zero for cylindrical folds and monocline. (Bergbauer&Pollard, 2003)

The Gaussian curvature was calculated on Skua-Gocad for the whole structural grid volume (Fig. 45). From this calculation many zones of the structure with non-zero Gaussian curvature are identified.

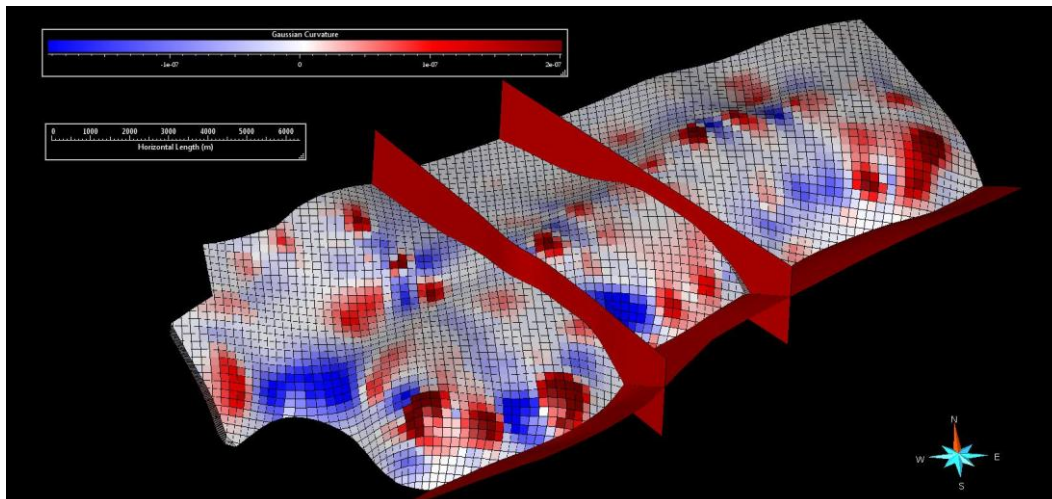


**Fig 45:** The Gaussian curvature of the Col Visentin – Monte Garda anticline within the VOI. Here, the curvature was measured on the surface corresponding to the top of Vajont Oolitic Limestone. The red surfaces are the faults-network.

### 5.3 Geostatistical distribution of the dolomitization

The available data on the dolomitization front are in the form of stratigraphic heights above or below the boundary between the Vajont Oolitic Limestone and the Fonzaso Formation.

These are highly unevenly distributed because they could only be retrieved in the field close to the outcrops of the boundary. Therefore, a geostatistical method was used to extend the dolomitization front on the whole VOI.

The simple Kriging is used generally for the data that have no-spatial trend of its distribution and the mean of data is constant and known. In Skua Gocad the points that are out of the range of the variogram, the Kriging algorithm automatically assigns to it the global mean value.

A simple Kriging method was chosen to evaluate the dolomitization distribution in our model, assuming the following formula:

$$Z(s) = \mu + \varepsilon(s)$$

where  $Z(s)$  stands for a general unknown point position,  $\mu$  for the exact mean of data and  $\varepsilon(s)$  for the distance between  $Z(s)$  and  $\mu$ . In figure 46, the data are given by the solid circles.

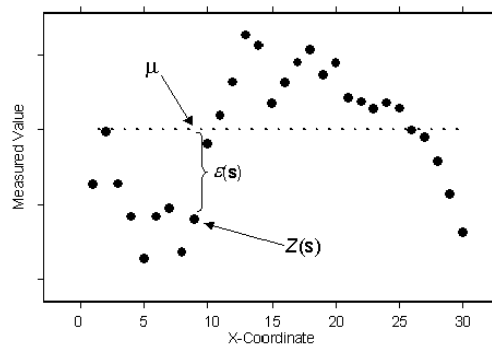


**Fig 46:** Data distribution about the mean value  $\mu$  associated to the a general distance value  $\varepsilon(s)$

The data used for the simple Kriging are the geographical positions where the top of the dolomitization was detected in the field. From these data, the stratigraphic distances between the dolomitization front and the top of the Vajont Oolitic Limestone were calculated (Fig. 47).

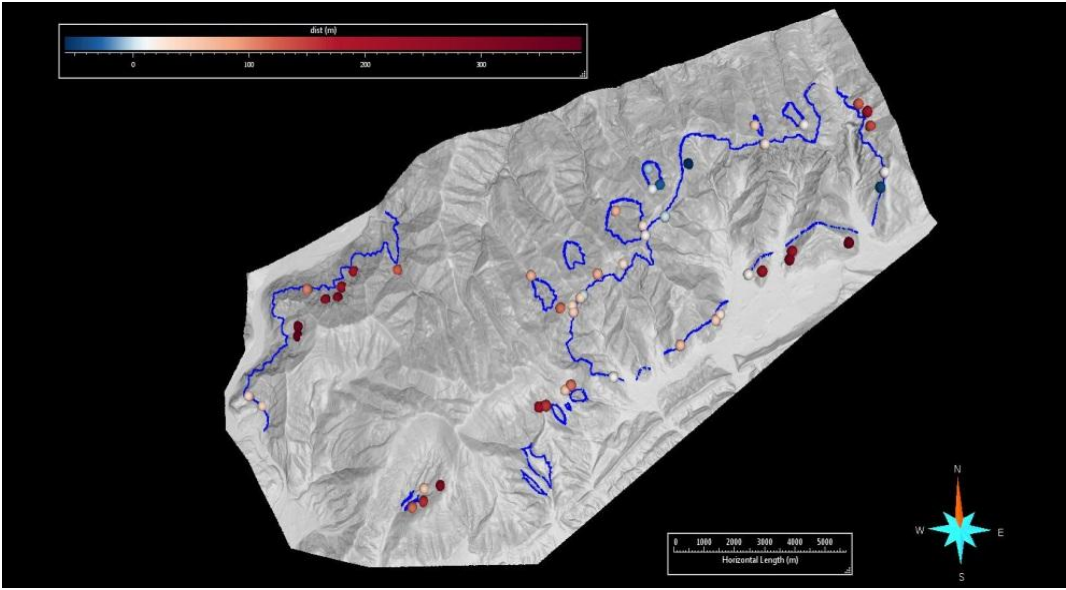


**Fig 47:** The pointset, by the chromatic scale shows the distance of the dolomitization front from the upper Vajont Oolitic Limestone boundary highlighted in blue, within the VOI box-set.

The distribution of the top of dolomitization with respect the Vajont Oolitic Limestone as obtained from simple Kriging, is shown in figure 48.

Three areas can be highlighted where the dolomitization front reached a stratigraphic level far above of the top of the Vajont Oolitic Limestone and two areas were the dolomitization front remained well below the top of the Vajont Oolitic Limestone.

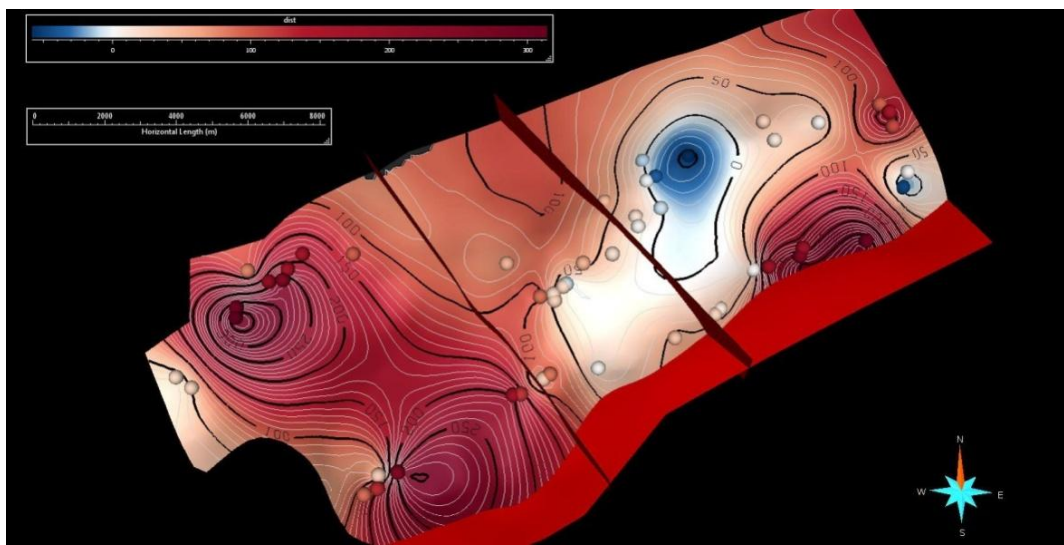


**Fig 48:** Stratigraphic heights reached by the dolomitization above the top of the Vajont Oolitic Limestone as resulted from simple Kriging.

## 5.4 The 3D representation of the dolomitization front

The result of Kriging interpolation was thus the distribution of stratigraphic distances of the dolomitization front from the boundary between the Vajont Oolitic Limestone and the Fonzaso Formation. A new pointset was created which points are translated from the top of the Vajont Oolitic Limestone by a value equal to the Kriging results, along their stratigraphic normal (Fig. 49). This new pointset was used to build the dolomitization front surface.

The dolomitization front surface was compared to the dolomitization front mapped during the survey, and show a good agreement (Fig. 50).

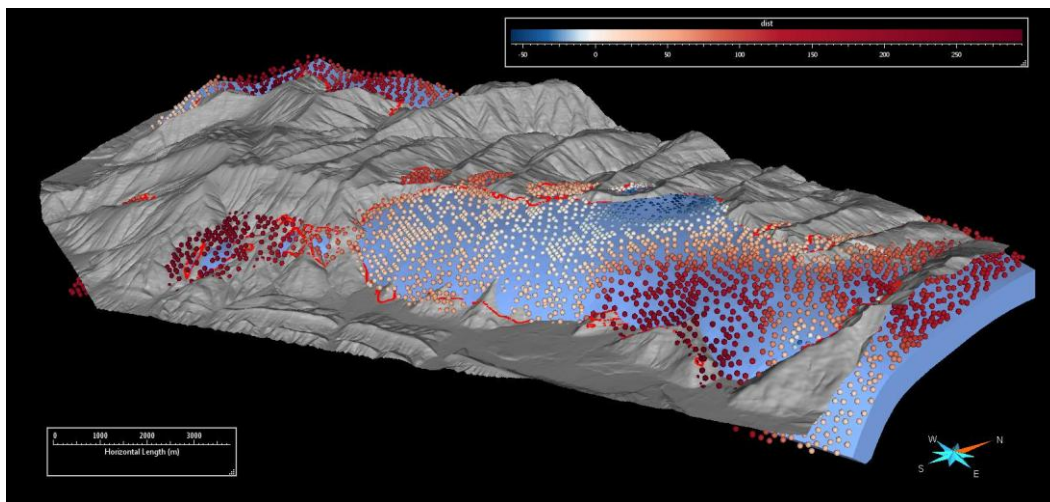


**Fig 49:** Pointset depicting the dolomitization front. The different colour of the pointset represent the distance from the top of the Vajont Oolitic Limestone. The blue color stands for negative highs, while the red color for positive values (i.e., the dolomitization front is within the Fonzaso Formation)

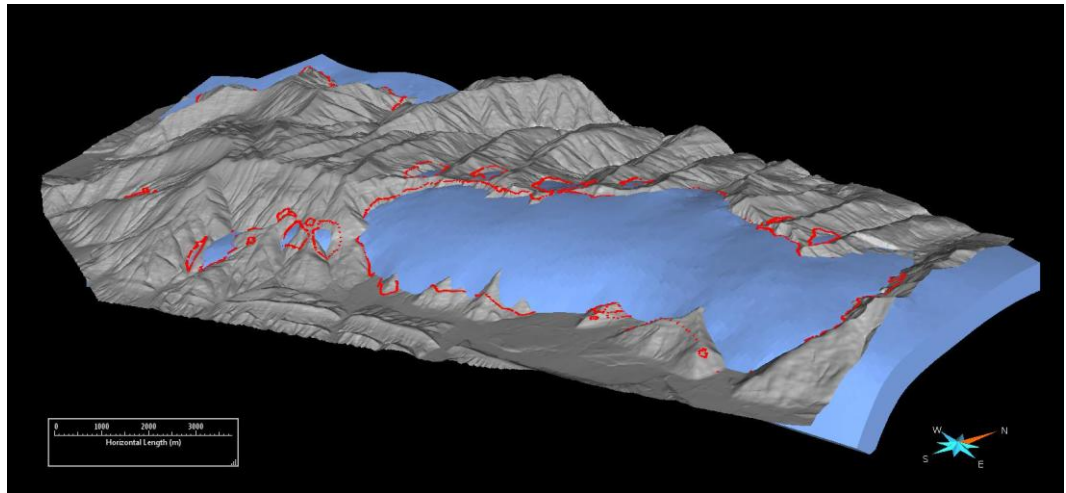


**Fig 50:** The red line is the mapped dolomitization front plotted on the mesh of the structure, the blue volume is the Vajont Oolitic Limestone.

The surface thus created (Fig. 51) shows the validity of this geostatistical data interpretation, because the surface of dolomitization fits the dolomitization boundaries mapped during the survey.

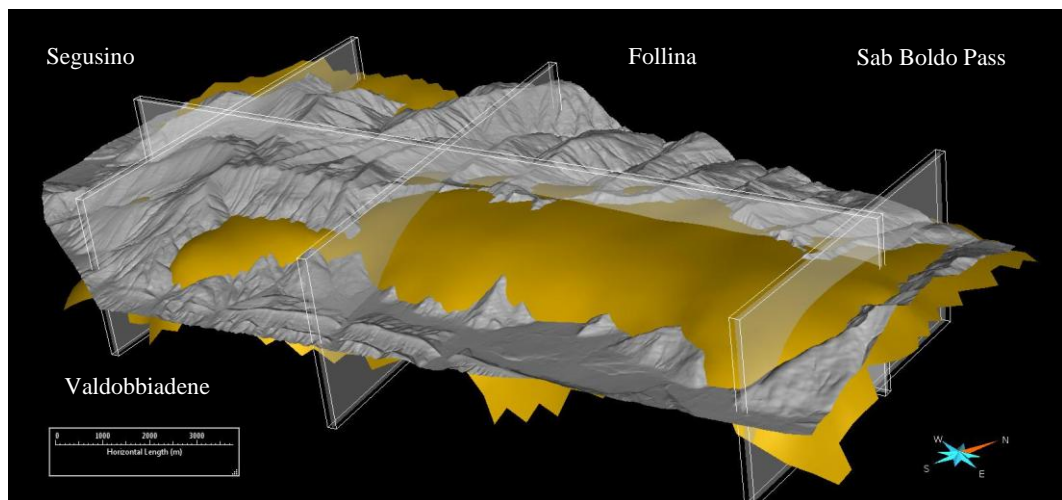


**Fig 51:** The yellow surface represents the distribution of the dolomitization front on the Col Visentin – Monte Garda anticline, with the four cross sections also represented (see Fig 52-55).

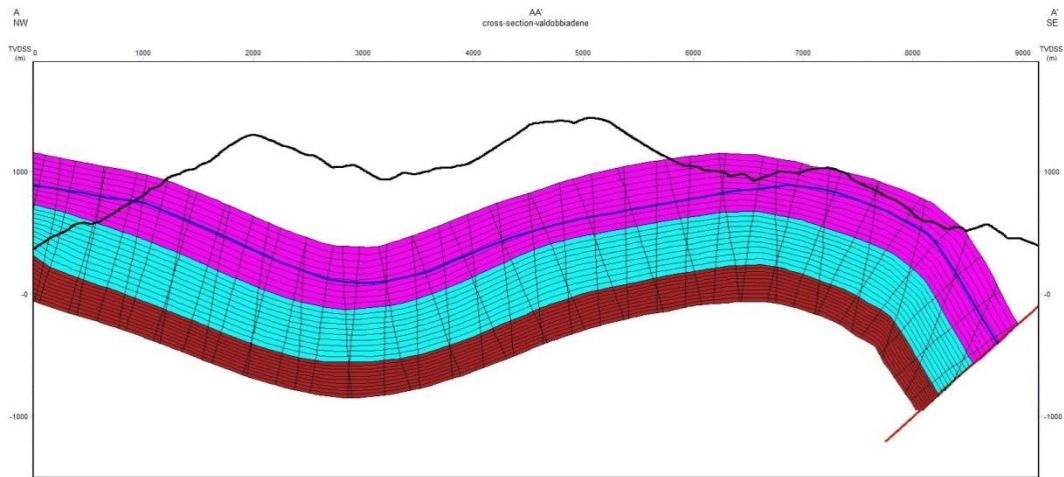


**Fig 52:** The Valdobiadene cross section, blue line: top of dolomitization, pink: Fonzaso Formation, blue: Vajont Oolitic Limestone red: Igne Formation, the dark brown surface to the SE° is the Bassano-Valdobiadene thrust.

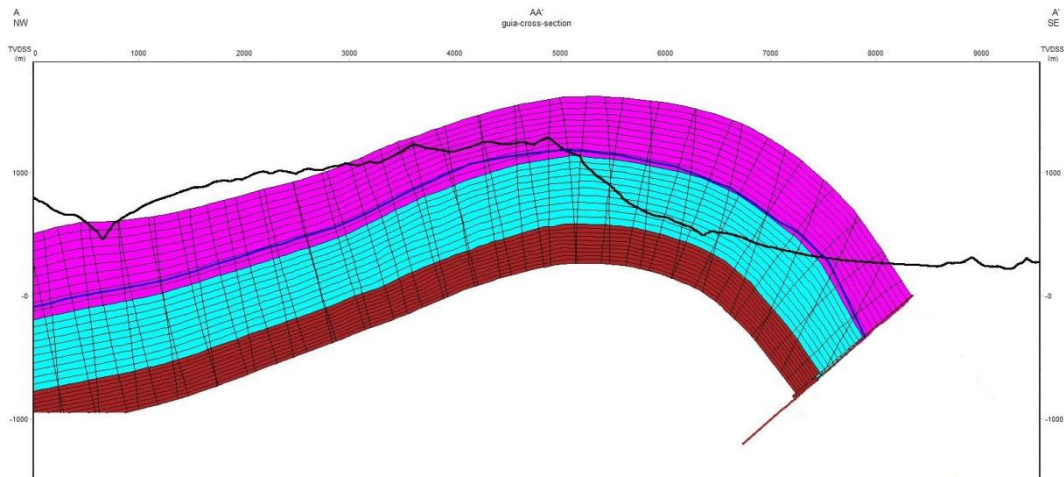


**Fig 53:** The Valdobiadene cross section, blue line: top of dolomitization; pink: Fonzaso Formation; blue: Vajont Oolitic Limestone; red: Igne Formation; the dark brown surface to the SE° is the Bassano-Valdobiadene thrust.



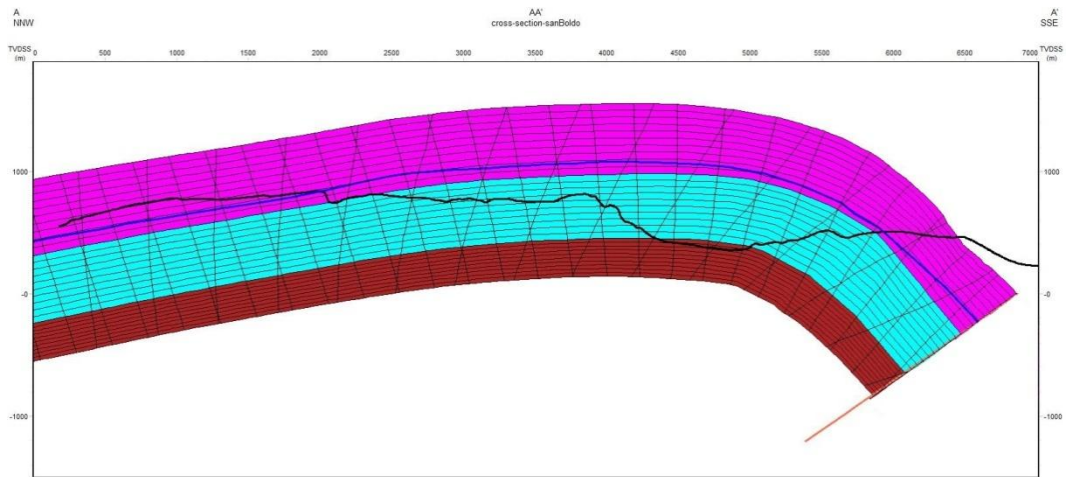


**Fig 54:** The Valdobbiadene cross section. Blue line: top of dolomitization; pink: Fonzaso Formation; blue: Vajont Oolitic Limestone; red: Igne Formation; the dark brown surface to the SE<sup>o</sup> is the Bassano-Valdobbiadene thrust.

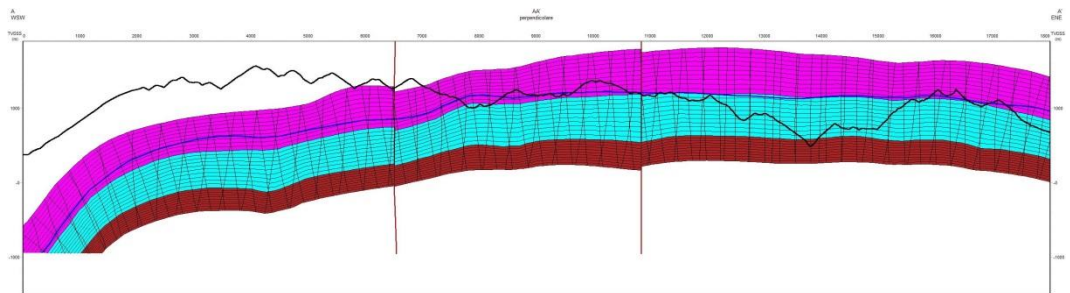


**Fig 55:** The Valdobbiadene cross sections. Blue line: top of dolomitization; pink: Fonzaso Formation; blue: Vajont Oolitic Limestone; red: Igne Formation; the dark brown surface to the SE<sup>o</sup> is the Bassano-Valdobbiadene thrust.

## 5.5 Volume of dolomitized rock

The same process used for the grid volumes construction described in the 5.1.3 paragraph was used to estimate the total volume of the dolomitized rocks (Fig. 56). This volume was calculated using the upper Igne Formation boundary (Fig. 32) for the base and the dolomitization surface (Fig. 51) for the top of the dolomitized rock body within the VOI.

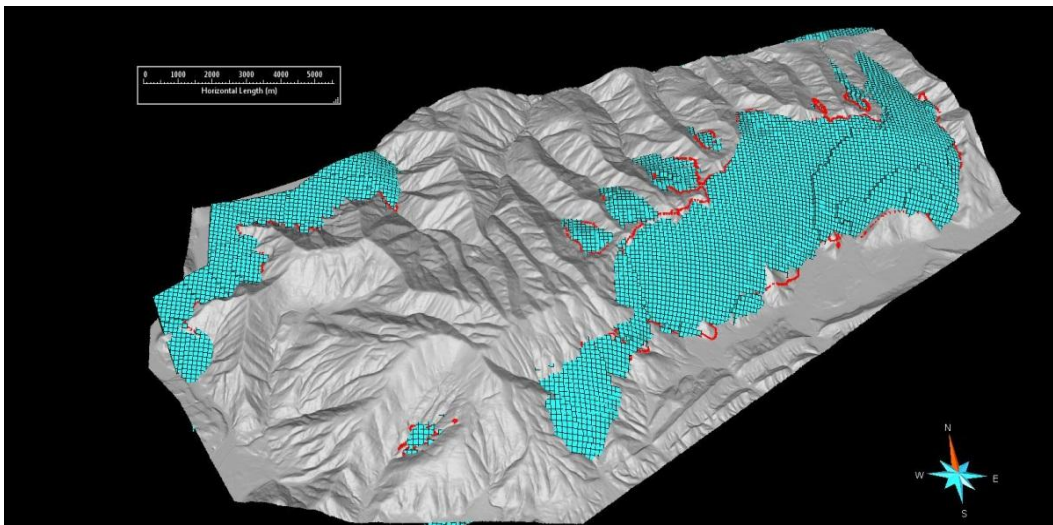


**Fig 56:** The total volume calculated of the dolomitizing rocks, the red lines on the mesh surface are the mapped dolomitization boundary.

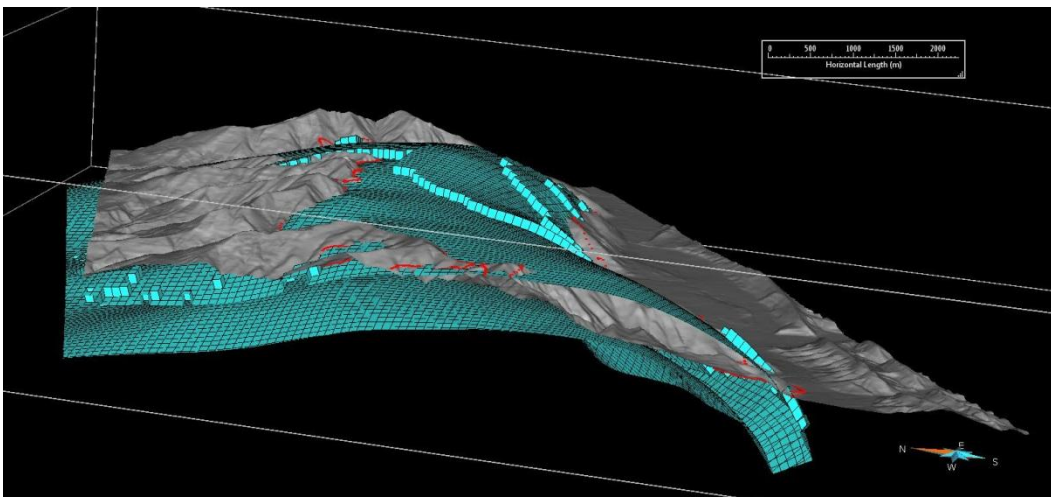


**Fig 57:** A section of the eastern portion of the Col Visentin - Monte Garda anticline, view from NE.

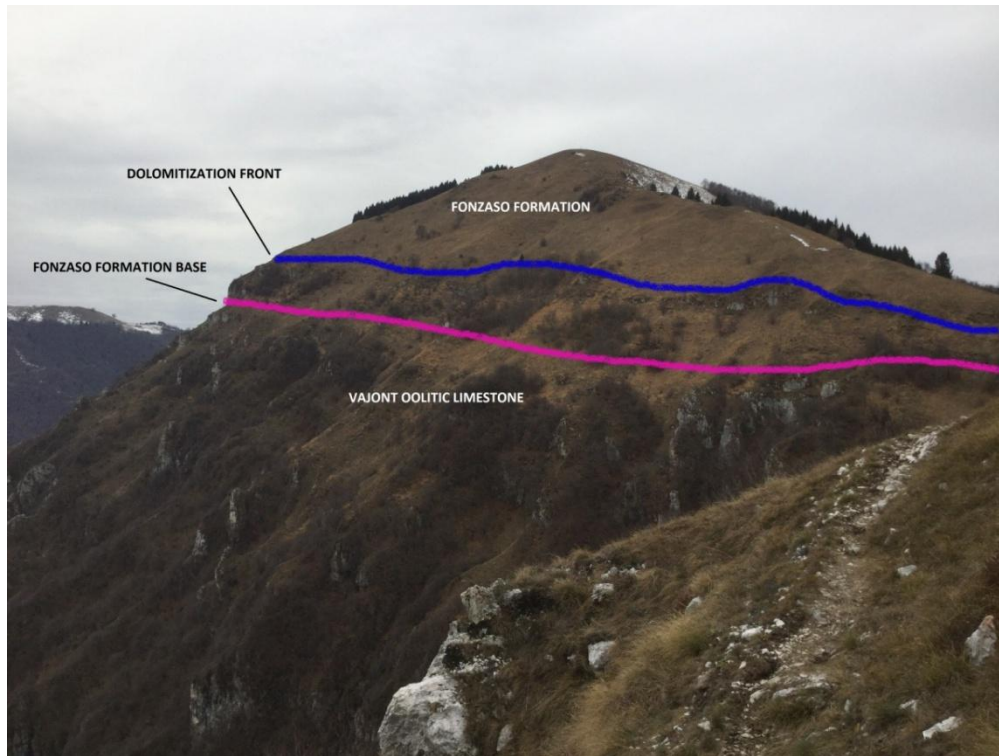


**Fig 58:** Picture from the eastern part of the Col Visentin - Monte Garda anticline, near San Boldo Pass. The pink line coincides with the upper Vajont Oolitic Limestone boundary, the blue line is the dolomitization front, which here extended across the Fonzaso Formation.

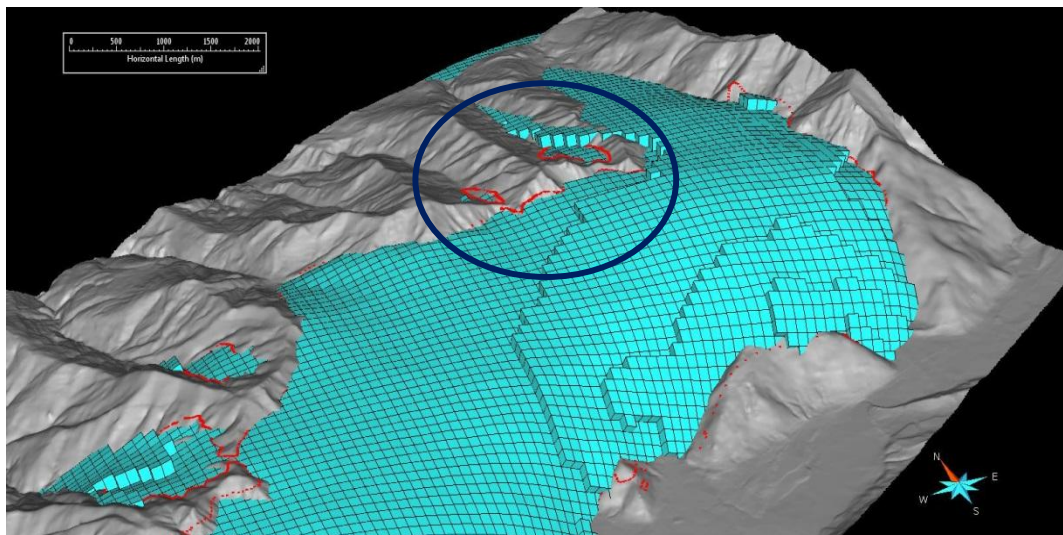


**Fig 59:** Detail of the dolomitization volume, the blue circle encloses the area shown in figure 59. Red line: mapped dolomitization front; blue voxets: reconstructed dolomitized volume.

As conclusion of the work, a 3D model of the dolomitization volume was built. Even if the Igne Formation shows dolomitization in a few outcrops on the Col Visentin - Monte Garda anticline, we didn't consider it to calculate the dolomitization volume and we used the lower Vajont Oolitic Limestone as boundary. The following table shows the dolomitized volumes of the Vajont Oolitic Limestone, the Fonzaso Formation and the Maiolica, with their percentage of dolomitization.

Table of dolomitized rocks volumes		
Formation	Dolomitization Volume	Percentage
Vajont Oolitic Limestone	85.816x10 <sup>9</sup> m <sup>3</sup>	99.86%
Fonzaso	21.084x10 <sup>9</sup> m <sup>3</sup>	21.04%
Maiolica		0%
Total	104.534x10 <sup>9</sup> m <sup>3</sup>	

**Table 2:** The dolomitized rock volumes.

## **6 Discussion**

### **6.1 Dolomitization/Faults relationships**

The reconstructed dolomitization front of the Col Visentin - Monte Garda anticline shows different zones where the dolomitization reached different stratigraphic heights. As described earlier, there are three main zones where the dolomitization front was detected 250 m – 300 m above the top of the Vajont Oolitic Limestone, while on the contrary two areas were found where the dolomitization front is 50 m below the boundary, as can be seen in figure 49.

The two areas with the maximum distance between the dolomitization front and the top of the Vajont Oolitic Limestone are located on the western portion of the Col Visentin - Monte Garda anticline, along the Quero Valley, another one is located in the eastern portion of the structure, close to the Bassano - Valdobbiadene thrust. The Kriging distribution of the dolomitization, shown in figure 48, can suggest some relationships between the dolomitization and the faults network.

In a typical foreland wedge-top and in the context of a squeegee type of dolomitization we expect the fluids to spread along the basal thrust faults and then propagate along the other principal faults.

In this case study, the dolomitization along the Bassano - Valdobbiadene thrust seems to have been uneven. Figure 48 shows a low stratigraphic elevation of the dolomitization front in the area between the Follina and the Combai faults.

The Combai and the Follina faults have NNW - SSE strike direction. These two faults have the same strike direction of the Quero strike-slip fault, which is related to the reactivation of Mesozoic rifting faults (Fig. 37).

The Combai and Follina faults have probably been triggered by differential compressive forces active in the area of study during the Neo-Alpine event. The compression is demonstrated by the Bassano – Valdobbiadene thrust and by the Col Visentin – Monte Garda anticline. Here, compressive forces probably resulted in strong deformation which modified the thickness of some formations. This relation is particularly expressed within the Cretaceous succession. The Maiolica and Scaglia Variegata Alpina, being composed by thin layers with silt-clay intercalations are more deformable and formed parasitic folds, of the Z-S type for the limbs and of the M type for the hinge portion of the Col Visentin - Monte Garda anticline (Fig. 20).

The portion of the Col Visentin - Monte Garda anticline near the Follina fault shows a uniform and low stratigraphic elevation of the dolomitization front. The relative low dolomitization in this area could suggest that the Follina fault didn't exist during the spreading of dolomitizing fluids, for this reason it could be dated as a post Oligocene-Neogene compression event. An alternative scenario implies the Follina fault zone had permeability. This last interpretation was favoured.

The area on the Col Visentin - Monte Garda near the Combai fault shows a large variation of the dolomitization front (Fig. 48). Dolomitizing fluids may have used the Combai fault to spread above the Vajont Oolitic Limestone. This implies that during the dolomitization the Combai fault was permeable.

In the western portion of the Col Visentin - Monte Garda anticline, the maximum height of the dolomitization front was reached.

Indeed, this area corresponds to a direction change of the fold axis from ENE - WSW to NW-SE. Most probably this change of the axis direction is due to the activity of the Quero fault, which should have had a transpressive behaviour during the Neo-alpine phase. The Quero fault could have concentrated most of the dolomitizing fluids in this portion of the Col Visentin - Monte Garda anticline.

In this scenario the Follina fault would have worked as a seal for the eastward distribution of the dolomitizing fluids, this explains the relative low dolomitization in east portion, close to the Follina fault.

Another scenario invokes the presence of a blind fault, below the zone of the highest dolomitization and in correspondence with the fold axial change located in the western portion of the Col Visentin - Monte Garda anticline. The Kriging map shows a NW - SE trend of the dolomitization distribution corresponding with the main strike of the Combai and Follina faults. Since this is the strike of inherited Mesozoic faults, it is possible that this alignment of stronger dolomitization may mimic the trace of a buried Mesozoic fault.

There is no direct surface evidence of such a fault, however some elements may let us suppose the influence of ancient lineaments on the development of the lateral ramp responsible for the deflection of the Col Visentin - Monte Garda anticline axis.

The study area in the Early Jurassic was located near the transition-zone between the Trento Platform and the Belluno Basin. The Trento Platform was bounded to by an escarpment coinciding with approximately NNW-SSE trending normal faults.

## 6.2 Detection of a blind back thrust in the NE sector

From the 3D model of the Col Visentin - Monte Garda anticline, it has been possible to identify the presence of a blind back thrust, located behind the hinge of the fold and which does not crop out. A back thrust has been mapped close to the San Boldo Pass, just outside the study area (F.N 063 Belluno,1996, scale 1:50.000).

This structure does not crop out in the study area but a pair of strongly asymmetric folds is found (Fig. 43) on the continuation of the back thrust mapped in the Belluno sheet, which we interpreted as the surface expression of the thrust becoming a blind thrust towards the West.

The presence of the blind back thrust, associated to the Bassano - Valdobbiadene frontal thrust, implies a pop-up geometry of the Col Visentin - Monte Garda anticline (Fig. 60).

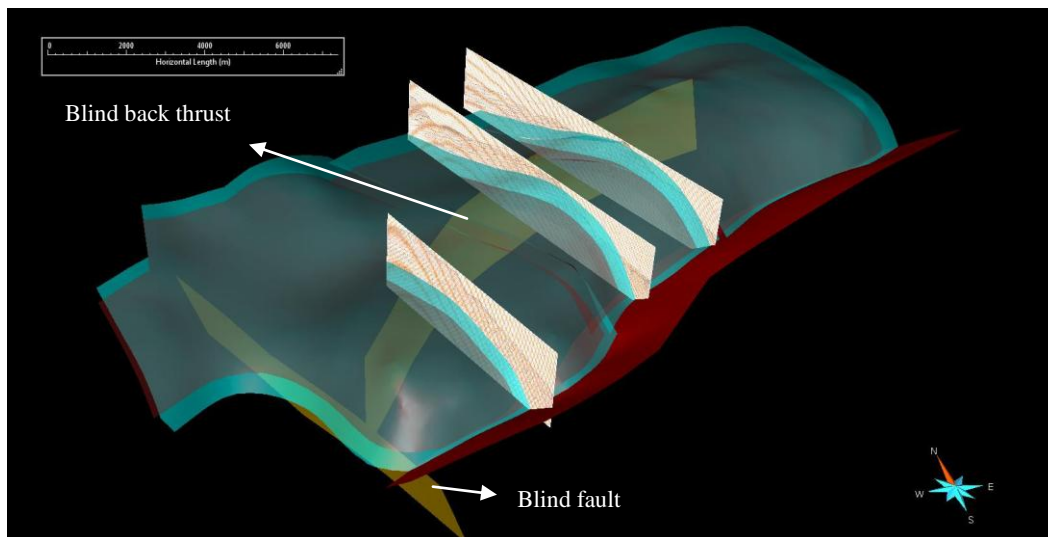
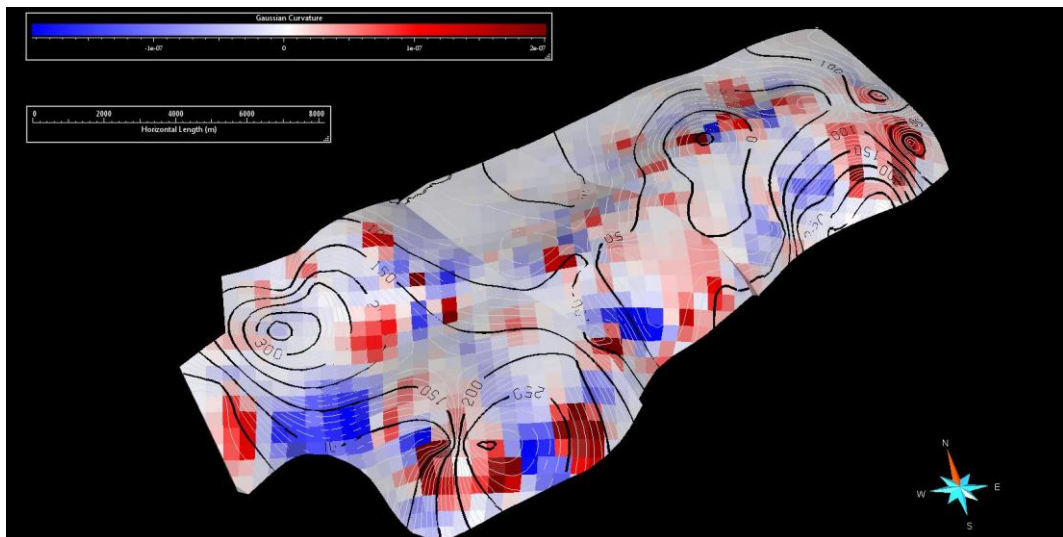


**Fig 60:** The position of the blind back-thrust on the north-east and the supposed blind fault on the west near Quero Valley.



### 6.3 Gaussian curvature and dolomitization

The relationships between the areas with the maximum value of the Gaussian curvature and the elevation of the dolomitization front were investigated. The areas where the maximum Gaussian curvature has been calculated might present the maximum value of fracturing, and thus they could be for the regions with maximum dolomitization. Such a correlation however, is not evident in the whole structure, since some strongly dolomitized portions have no correlation with areas with large values of the Gaussian curvature (Fig. 61). There are, however, two regions in which the dolomitization front reached high stratigraphic elevations and which coincide with portions of the Col Visentin - Monte Garda anticline with the highest values of Gaussian curvature. These two regions are both located near the Bassano - Valdobbiadene thrust, where the structure is more or less intensely deflected. A third region of high elevation of the dolomitization front (NW portion of the study area) is instead not related to a strong Gaussian curvature. This region is close to the Quero fault, i.e., two structural elements with different age interact near the region of strong dolomitization.

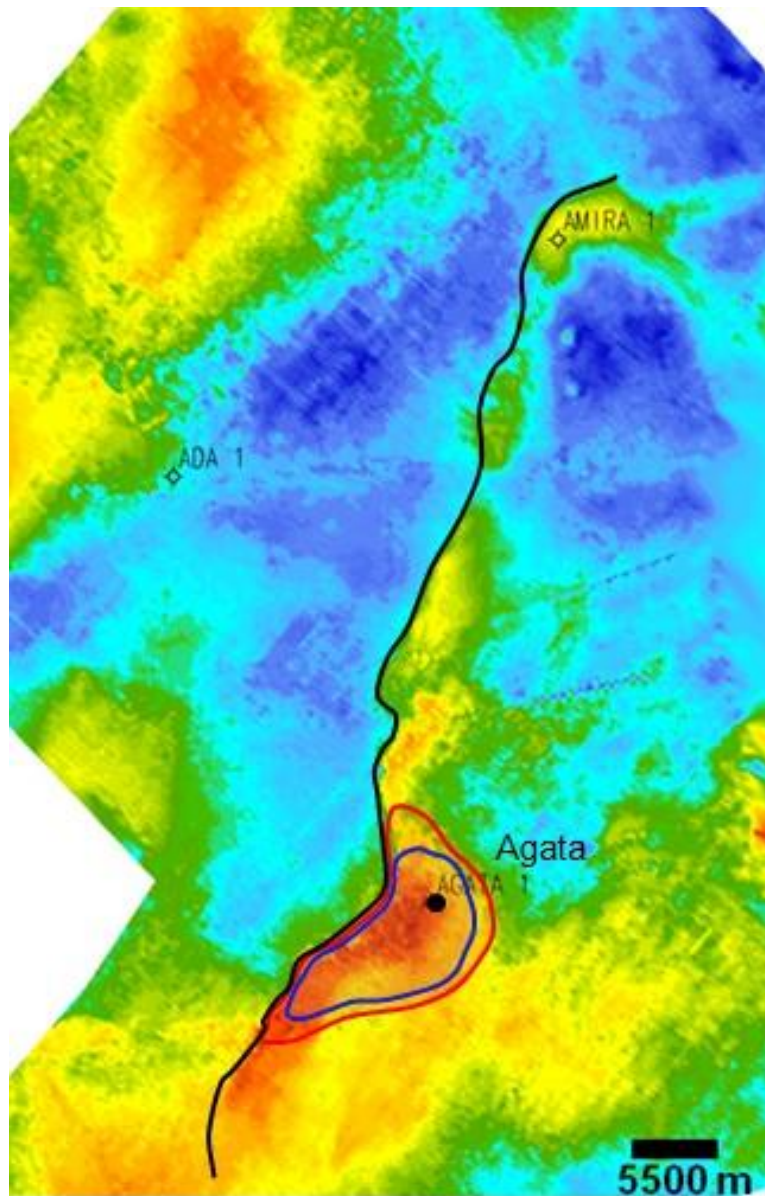


**Fig 61:** The contour shows the top of the dolomitization front plotted on the Gaussian curvature of the Vajont Oolitic Limestone grid volume (400mx400m cells areal size), the red cells (positive Gaussian curvature) could represent the area of the Col Visentin – Monte Garda anticline that have been subjected to the highest fracturation.




## **6.4 Comparison with analog structure in the subsurface**

The Col Visentin – Monte Garda anticline happens to have nearly the same scale, and to be affected by a similar volume of dolomitization of the Agata buried structure in the northern Adriatic foreland (Northern Italy) studied by ENI e&p division. The structure is a culmination of a anticline fold developed along a NNE trending, ESE dipping Dinaric reverse fault which reactivated older Mesozoic extensional faults. This inversion structure is characterized by the presence of two culminations, Amira to the north and Agata located to the south. The isopach data show how the growth of the Agata culmination was more pronounced.

Seismic absorption was calculated and has been used to identify the dolomitization for the area of interest. Dolomitization reached higher at fold culminations, but while the Agata culmination shows dolomitization that affected the whole Mesozoic carbonate succession from the Calcarei Grigi Group (Lower Jurassic) up to the pelagic Scaglia (Middle Eocene), in the Amira culmination the dolomitization only reached the pelagic Maiolica (Lower Cretaceous). The interpretation is that dolomitizing fluids, mobilized during the Cenozoic compression, were focused into the Agata culmination because of stronger fracturation.



**Fig 62:** Isopach maps of the Scaglia in the Adriatic subsurface near the Agata and Amira culminations (courtesy of ENI S.p.a: from Fantoni et al., 2014). This rendering shows the different subsidence rates of regions close to the Dinaric reverse fault during the Eocene. The red polygon encloses the portion of Maiolica that was dolomitized, while the blue polygon encloses the dolomitized portion of the Scaglia.

-  Maiolica dolomitization (Upper Cretaceous)
-  Scaglia dolomitization (Middle Eocene)
-  Basin Inversion

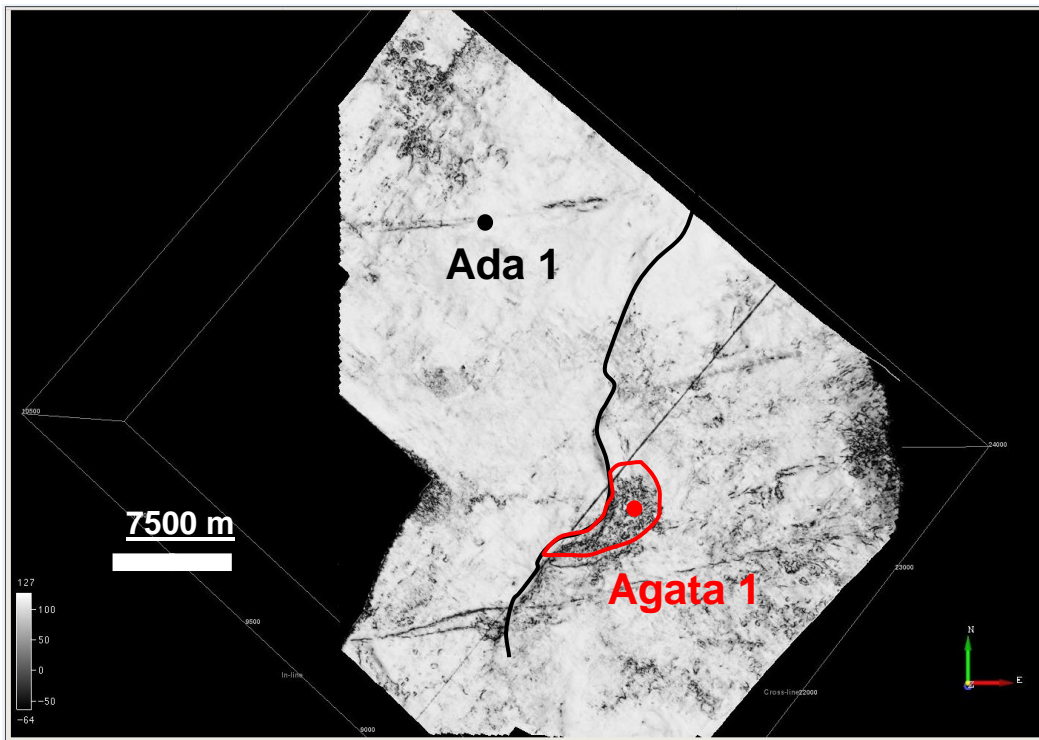


**Fig 63:** Courtesy of ENI S.p.a., The top Scaglia continuity extraction map. The red polygon encloses the zone where the maximum dolomitization was identified into the Scaglia lithology.

The Agata structure could be compared with the Col Visentin - Monte Garda anticline, because both structures are in the order of kilometres, and both are non-cylindrical folds, with axial culminations and depressions. The dolomitization in the Agata structure was described as pervasive on the whole culmination (Fig. 65), for the entire Mesozoic carbonate succession (Fig 62), while in the Col Visentin – Monte Garda anticline the dolomitization is generally hosted in the Vajont Oolitic Limestone with positive spatial variations of its top. Figure 63 shows how the maximum dolomitization was individuated in the portion located on the axial deflection. The same characteristics were found in the Col Visentin - Monte Garda anticline, where the area of axial deflection exhibits the maximum height of dolomitization. The Agata culmination is characterized by the presence of a old buried fault, that has permitted the diffusion of the dolomitizing fluids across the lithostratigraphic units, reaching the upper Scaglia boundary.

The same process, i.e., the interaction of a Cenozoic compressive structure with a inherited extensional fault, could explain the highest dolomitization for the Col Visentin - Monte Garda anticline near the Quero fault. The Agata culmination was formed by Dinaric compression, whereas the Col Visentin - Monte Garda was formed during the Neo-Alpine compression. Despite the different age and orientation, however, the dolomitization front seem to have reached the highest stratigraphic elevations, in both cases, where the most recent compressional structure interacted with an inherited Mesozoic extensional fault or alignment.

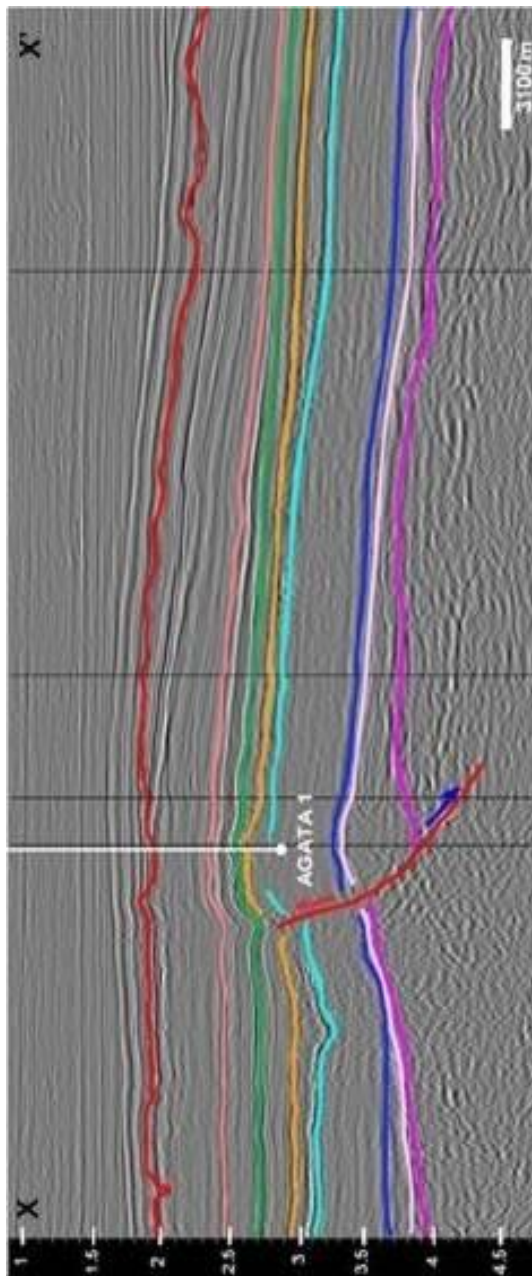


**Fig 65:** A seismic section interpreted from ENI. Yellow reflector: top Maiolica, green reflector: Scaglia, pink reflector: Base Oligocene

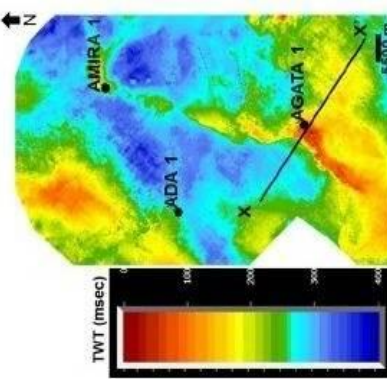


**Fig 64:** From ENI, isopach map, x-x', cross section line

## 7 Conclusion

The main goal of this work of thesis has been the reconstruction of the dolomitization front within the Col Visentin - Monte Garda anticline. In order to achieve this purpose, a multi-method approach, including geological mapping, 3D geo-modelling and geostatistics has been used.

The produced geological map allows to recognize the main fault lines. The fold shows a deflection of its axis from ENE - SWS to SE - NW near the locality of Valdobbiadene (TV).

From the 3D geological model the geometries and volumes of rock bodies were extracted. Furthermore, the 3D representation permitted to visualize the culminations and the depressions of the fold. From the 3D model, it has been possible to recognize a blind back thrust located behind the fold hinge in continuity with a back thrust, known from literature, that occurs close to the San Boldo Pass. Relationships between pre-Alpine faults and the Alpine anticline structure have been established. In fact the axial deflection in the western portion of the Col Visentin - Monte Garda anticline has been directly related to the Quero strike-slip fault. The Vajont Oolitic Limestone is entirely dolomitized, excluded in some portions, in the Col Visentin - Monte Garda anticline. The spreading of the dolomitizing fluids into it might have been related to some primary porosity. The underlying Igne Formation instead is only partially dolomitized, presumably only in fracture zones that have permitted the fluids upwelling.

The stratigraphic units above the Vajont Oolitic Limestone can be dolomitized, and the stratigraphic height reached by the dolomitization has been considered as a measure of how intense the dolomitization has been. This work highlighted that the dolomitization may have been more intense where the fold axis is deflected, and the relationship found between the dolomitization and the fault network could be helpful to improve the knowledge of the dolomitization distribution along the axis deflections in subsurface analogues.

There is in fact some relationship between the Gaussian curvature and the areas with the highest dolomitization. These areas could have corresponded with the maximum fracturing of the rocks, which may have improved its porosity and permeability (Murray 1968).

## 8 Bibliography

- Bergbauer, S., Pollard, D.D., 2003. How to calculate normal curvatures of sampled geological surfaces. *J. Struct. Geol.* 25, 277–289. [https://doi.org/10.1016/S0191-8141\(02\)00019-6](https://doi.org/10.1016/S0191-8141(02)00019-6)
- Bistacchi, A., Balsamo, F., Storti, F., Mozafari, M., Swennen, R., Solum, J., Tueckmantel, C., Taberner, C., 2015. Photogrammetric digital outcrop reconstruction, visualization with textured surfaces, and three-dimensional structural analysis and modeling: Innovative methodologies applied to fault-related dolomitization (Vajont Limestone, Southern Alps, Italy). *Geosphere* 11, 2031–2048. <https://doi.org/10.1130/GES01005.1>
- Bondesan A., Busoni S., Preto N.(2011). Carta geologica delle provincia di Treviso. Sezioni 084030 - Tarzo 063150 - Passo di San Boldo, scala 1:10.000.
- Bondesan A., Busoni S., Preto N.(2011). Carta geologica delle provincia di Treviso. Sezioni 084040 - Vittorio Veneto, scala 1:10.000.
- Bondesan A., Busoni S., Preto N.(2011). Carta geologica delle provincia di Treviso. Sezioni 084010 - Monte Garda 084050 - Combai, scala 1:10.000.
- Bondesan A., Busoni S., Preto N.(2011). Carta geologica delle provincia di Treviso. Sezioni 084020 - Follina 063140 - Ponte Valmaor, scala 1:10.000.
- Bondesan A., Busoni S., Preto N.(2011). Carta geologica delle provincia di Treviso. Sezioni 083080 - Segusino 083040 - Marzai, scala 1:10.000.
- Burrato, P., Poli, M.E., Vannoli, P., Zanferrari, A., Basili, R., Galadini, F., 2008. Sources of Mw 5+ earthquakes in northeastern Italy and western Slovenia: An updated view based on geological and seismological evidence. *Earthq. Geol. Methods Appl.* 453, 157–176. <https://doi.org/10.1016/j.tecto.2007.07.009>
- Caputo, R., Poli, M.E., Zanferrari, A., 2010. Neogene–Quaternary tectonic stratigraphy of the eastern Southern Alps, NE Italy. *J. Struct. Geol.* 32, 1009–1027. <https://doi.org/10.1016/j.jsg.2010.06.004>
- Casati, P. & Tomai, M. (1969) - Il Giurassico e il Cretacico nel versante settentrionale del vallone bellunese e del gruppo del M. Brandol, *Ric. It. Pal. Strat.*, 75 (2): 205 - 340, 33 figg. Milano.
- Castellarin, A., Cantelli, L., 2000. Neo-Alpine evolution of the Southern Eastern Alps. *J. Geodyn.* 30, 251–274. [https://doi.org/10.1016/S0264-3707\(99\)00036-8](https://doi.org/10.1016/S0264-3707(99)00036-8)
- Castellarin, A., Nicolich, R., Fantoni, R., Cantelli, L., Sella, M., Selli, L., 2006. Structure of the lithosphere beneath the Eastern Alps (southern sector of the TRANSALP transect). *Tectonophysics, TRANSALP* 414, 259–282. <https://doi.org/10.1016/j.tecto.2005.10.013>
- CHOQUETTE PHILIP W., HIATT ERIC E., 2007. Shallow- burial dolomite cement: a major component of many ancient sucrosic dolomites. *Sedimentology* 55, 423–460. <https://doi.org/10.1111/j.1365-3091.2007.00908.x>



- Cosgrove, J.W., Ameen, M.S., 1999. A comparison of the geometry, spatial organization and fracture patterns associated with forced folds and buckle folds. *Geol. Soc. Lond. Spec. Publ.* 169, 7. <https://doi.org/10.1144/GSL.SP.2000.169.01.02>
- Di Cuia, R., Riva, A., SCIFONI, A., MORETTI, A., SPÖTL, C., Caline, B., 2011. Dolomite characteristics and diagenetic model of the Calcarei Grigi Group (Asiago Plateau, Southern Alps - Italy): An example of multiphase dolomitization. <https://doi.org/10.1111/j.1365-3091.2010.01212.x>
- Doglioni, C., 1987. Tectonics of the Dolomites (southern alps, northern Italy). *J. Struct. Geol.* 9, 181–193. [https://doi.org/10.1016/0191-8141\(87\)90024-1](https://doi.org/10.1016/0191-8141(87)90024-1)
- Doglioni, C., Bosellini, A., 1987. Eoalpine and Mesoalpine tectonics in the Southern Alps. <https://doi.org/10.1007/BF01821061>
- Fantoni, R., Dal Zotto, O., Fattorini, A., Martinis, S & Stanculete, A., 2014. Inversion structure in the Po Plain and Adriatic foreland (Northern Italy).
- F. Sibley, D., Gregg, J., 1987. Classification of Dolomite Rock Texture.
- Gattolin, G., Preto, N., Breda, A., Franceschi, M., Isotton, M., Gianolla, P., 2015. Sequence stratigraphy after the demise of a high-relief carbonate platform (Carnian of the Dolomites): Sea-level and climate disentangled. *Palaeogeogr. Palaeoclimatol. Palaeoecol.* 423, 1–17. <https://doi.org/10.1016/j.palaeo.2015.01.017>
- Gregg Jay M., Bish David L., Kaczmarek Stephen E., Machel Hans G., 2015. Mineralogy, nucleation and growth of dolomite in the laboratory and sedimentary environment: A review. *Sedimentology* 62, 1749–1769. <https://doi.org/10.1111/sed.12202>
- J. Lucia, F., 2004. Origin and petrophysics of dolostone pore space. <https://doi.org/10.1144/GSL.SP.2004.235.01.06>
- Machel, H.G., 2004. Concepts and models of dolomitization: a critical reappraisal. *Geol. Soc. Lond. Spec. Publ.* 235, 7. <https://doi.org/10.1144/GSL.SP.2004.235.01.02>
- Mancin, N., Cobianchi, M., Giulio, A.D., Catellani, D., 2007. STRATIGRAPHY OF THE CENOZOIC SUBSURFACE SUCCESSION OF THE VENETIAN-FRIULIAN BASIN (NE ITALY): A REVIEW. *Riv. Ital. Paleontol. E Stratigr. Res. Paleontol. Stratigr.* 113.
- Mancin N., Di Giulio A., Cobianchi M., 2009. Tectonic vs. climate forcing in the Cenozoic sedimentary evolution of a foreland basin (Eastern Southalpine system, Italy). *Basin Res.* 21, 799–823. <https://doi.org/10.1111/j.1365-2117.2009.00402.x>
- Martinelli, M., Franceschi, M., Massironi, M., Rizzi, A., Salvetti, G., Zampieri, D., 2017. An extensional syn-sedimentary structure in the Early Jurassic Trento Platform (Southern Alps, Italy) as analogue of potential hydrocarbon reservoirs developing in rifting-affected carbonate platforms. *Mar. Pet. Geol.* 79, 360–371. <https://doi.org/10.1016/j.marpetgeo.2016.11.002>
- Martins M., & Fontana M., 1968 - Ricerche sui calcari oolitici giurassici del Bellunese. *Ric. It. Pal. Strat.* 74 (4): 1177 - 1230, figg. 6 tav.

- Monegato G., Stefani C., Zattin M., 2010. From present rivers to old terrigenous sediments: the evolution of the drainage system in the eastern Southern Alps. *Terra Nova* 22, 218–226. <https://doi.org/10.1111/j.1365-3121.2010.00937.x>
- Ronchi, P., Masetti, D., Tassan, S., Camocino, D., 2012. Hydrothermal dolomitization in platform and basin carbonate successions during thrusting: A hydrocarbon reservoir analogue (Mesozoic of Venetian Southern Alps, Italy). *Mar. Pet. Geol.* 29, 68–89. <https://doi.org/10.1016/j.marpetgeo.2011.09.004>
- S.Alps.ThrustTectonics.1992.pdf, n.d.
- Santantonio, M., Carminati, E., 2011. Jurassic rifting evolution of the Apennines and Southern Alps (Italy): Parallels and differences. *Geol. Soc. Am. Bull.* 123, 468–484. <https://doi.org/10.1130/B30104.1>
- Sun, S., Hou, G., Zheng, C., 2017. Fracture zones constrained by neutral surfaces in a fault-related fold: Insights from the Kelasu tectonic zone, Kuqa Depression. *J. Struct. Geol.* 104, 112–124. <https://doi.org/10.1016/j.jsg.2017.10.005>
- Skua User Manuals 2015.2
- Structurally Complex Reservoirs. 292. ed. 2007. P
- Toscani, G., Marchesini, A., Barbieri, C., Di Giulio, A., Fantoni, R., Mancin, N., Zanferrari, A., 2016. The Friulian-Venetian Basin I: architecture and sediment flux into a shared foreland basin. *Ital. J. Geosci.* 135, 444–459. <https://doi.org/10.3301/IJG.2015.35>
- V. Costa., C. Doglioni., P. Grandesso., D. Masetti., G.B. Pellegrini., E. Tracanella. F.N 063 Belluno (Carta geologica d'Italia), anno 1996, scala 1:50.000.
- Warren, J., 2000. Dolomite: occurrence, evolution and economically important associations. *Earth-Sci. Rev.* 52, 1–81. [https://doi.org/10.1016/S0012-8252\(00\)00022-2](https://doi.org/10.1016/S0012-8252(00)00022-2)
- Zempolich, W.G., Hardie, L.A., 1997. Geometry of dolomite bodies within deep-water resedimented oolite of the Middle Jurassic Vajont Limestone, Venetian Alps, Italy: Analogs for hydrocarbon reservoirs created through fault-related burial dolomitization.
- Møller-Pedersen, P., & Koestler, A. G. 1997. Hydrocarbon seals: Importance for exploration and production. Amsterdam: Elsevier Science.

## 9 Thanks

Ho moltissime persone da ringraziare per questo traguardo raggiunto.

Ringrazio il Professore Nereo Preto che mi ha seguito e incoraggiato nella stesura di questo progetto, Marco Franceschi che mi ha insegnato l'utilizzo di Skua Gocad e mi è stato affianco dispensando preziosi consigli, inoltre vorrei ringraziare la dott.ssa Ornella Borromeo che ha sostenuto questo progetto con la partnership di ENI.

Un ringraziamento speciale va ai miei genitori. Grazie che mi avete dato la possibilità di studiare e di frequentare l'Università, avete permesso la realizzazione di questo mio sogno, ve ne sarò sempre grato, questo traguardo è anche merito vostro. Un pensiero va alla mia famiglia, a mio fratello Marcello e mia sorella Ginevra che mi hanno sempre sopportato e sostenuto, anche nei momenti più bui e alla mia nonna Anna che mi ha sempre voluto bene.

Un pensiero speciale va a te Caterina, la tua pazienza e il tuo amore sono stati indispensabili per me, soprattutto in questo periodo così carico di incertezze e di dubbi. Grazie.

Vorrei ringraziare i professori Anna Breda e Matteo Massironi che durante questi anni di università mi hanno dato preziosi consigli sulla strada da intraprendere e un ringraziamento va a Luca Collanega che mi ha sostenuto nei momenti difficili e si è dimostrato un amico.

Voglio ringraziare il mio amico Carlo e i miei coinquilini Stefano e Nicolas che mi hanno accompagnato durante i rilievi assieme a Caterina e alla Betzi.

Un grazie ai miei super coinquilini Stefano, Nicolas, Nicola, Filippo, Sara, Penelope e Miriam, avete reso la mia esperienza di vita a Padova ancora più bella.

Un grazie va a Mattia Martinelli, i tuoi consigli sono stati molto utili, da quando ti ho conosciuto mi hai aiutato tanto, sei un caro amico.

Voglio ringraziare i miei amici di sempre Flavio, Antonella, Pietro e Ilaria e al mio amico Davide Campostrini, grazie ragazzi che mi sopportate ormai da un bel po' di anni e non mi avete mai mandato a quel paese.

Voglio ringraziare i miei amici dell'Università in particolar modo Riccardo Inama, Edoardo Masiero, Michele Vallati e tutti gli altri che ho conosciuto ed apprezzato durante il mio percorso accademico, grazie a voi ho trascorso degli anni speciali qui a Padova e all'Università.

Ed infine un grazie speciale v`a alla mia Betzi, quanta strada abbiamo fatto assieme, nessuno avrebbe scommesso su di te, ed invece mi hai portato ovunque senza mai un problema. Sei la mia super macchina..

Grazie a tutti.